European Journal of Medicinal Chemistry 55 (2012) 228–242

Contents lists available at SciVerse ScienceDirect

European Journal of Medicinal Chemistry

journal homepage: http://www.elsevier.com/locate/ejmech

Original article

Discovery of 1-(β-amino substituted-β-alanyl)-*N*,*N*-dimethylindoline-2-carboxamides as novel nonpeptide antagonists of nociceptin/orphanin FQ receptor: Efficient design, synthesis, and structure–activity relationship studies

Shigeo Hayashi*, Katsuyo Ohashi, Eriko Nakata, Chie Emoto

Pfizer Global Research & Development, Nagoya Laboratories, Pfizer Japan Inc., 5-2 Taketoyo, Aichi 470-2393, Japan

ARTICLE INFO

Article history:
Received 7 May 2012
Received in revised form
11 July 2012
Accepted 15 July 2012
Available online 25 July 2012

Keywords:
Nociceptin/Orphanin FQ (N/OFQ)
NOP (ORL1) receptor antagonist
NOP receptor selectivity
Half-life in HLM

ABSTRACT

Since the discovery of endogenous nociceptin/orphanin FQ (N/OFQ) peptide and N/OFQ peptide (NOP) receptor [or opioid-receptor-like-1 (ORL1) receptor], the structures, distribution, and pharmacology have been reported in detail. N/OFQ and NOP receptor are located in the corticolimbic regions that are involved in the integration of the emotional activity, and located in the spinal cord, the peripheral nervous systems or other peripheral tissues that are related to pain as well as urinary signal transmissions, with a pattern distinct from that of classical opioid peptides and their receptors in rodents or primates. Furthermore, N/OFQ–NOP receptor system plays an important role in the regulation of various human physiologies such as depression effect, hyperphasia effect, and blood pressure effect. In this study, the structure–activity relationship of novel NOP receptor antagonist for various 1-(β-amino substituted-β-alanyl)-*N*,*N*-dimethylindoline-2-carboxamides was investigated *in vitro* to elucidate structural requisites to identify and develop potent and selective NOP receptor antagonists, which resulted in the discovery of 1-{3-[4-(substituted phenyl)piperidin-1-yl]propanoyl}-*N*,*N*-dimethylindoline-2-carboxamide analogues that display potent and selective human NOP (hNOP) receptor binding affinity and potent hNOP receptor antagonist activity. The efficient design, synthesis, and structure–activity relationship studies for potent and selective novel NOP receptor antagonists and significant findings *in vitro*, that include insights for binding and functional mechanisms via receptor–ligand interactions, are reported herein.

1. Introduction

An endogenous heptadecapeptide, nociception/orphanin FQ (N/OFQ[a]) [1a,b], and nociceptin/orphanin FQ peptide (NOP[1]) receptor [opioid-receptor-like-1 (ORL1) receptor or the fourth opioid peptide (OP4) receptor] [2a,b], that is a G-protein-coupled receptor (GPCR) and distinct from classical opioid peptide receptors despite their sequence similarities, are widely distributed in the corticolimbic regions involved in the integration of the emotional activity, and in the spinal cord, the peripheral nervous systems or other peripheral tissues related to pain as well as urinary signal transmissions [3a–i]. Significantly, N/OFQ has demonstrated the utilities of its agonist activity *in vivo* in various animal models, such as analgesic effect against neuropathic pain (chronic pain), acute pain or inflammatory pain in the peripheral and spinal cord [4a–m], anxiolytic effect [5a–i] as well as antianorectic effect [6a,b] in the brain. In fact, we have been reported the discovery of novel, highly selective and potent NOP receptor agonists, (i) HPCOM that demonstrates systemically potent and peripherally- and/or spinal cord-active/selective antiallodynic effect in animal peripheral neuropathic pain model, and (ii) MCOPPB that demonstrates orally potent and brain-active/selective anxiolytic effect in animal Vogel conflict model, in the distinct two series of drug-design, synthesis, and structure–activity relationship (SAR) studies by Hayashi et al., respectively [7,8a,b]. As well, it has been reported that N/OFQ displayed inhibitory effect on micturition reflex *in vivo* [9a], and attenuation effect on neurogenic detrusor overactivity without

Abbreviations: GPCR, G-protein-coupled receptor; N/OFQ, nociceptin/orphanin FQ; NOP receptor, N/OFQ peptide receptor [or opioid-receptor-like-1 (ORL1) receptor]; MOP receptor, μ-opioid peptide receptor; hNOP and hMOP receptors, human NOP and human MOP receptors, respectively; [^{35}S]GTPγS, [^{35}S]-guanosine 5′-(γ-thiotriphosphate); HEK, human embryonic kidney; CHO, Chinese hamster ovary; HLM, human liver microsome; WSCI, water soluble carbodiimide, that is, 1-ethyl-3-(3-dimethylaminopropyl)carbodiimide hydrochloride; HOBT, 1-hydroxybenzotriazole; SAR, structure–activity relationship; SMR, structure–metabolic stability relationship.

* Corresponding author.
E-mail address: Shigeo_Hayashi@nifty.com (S. Hayashi).

[1] Nomenclature Committee of the International Union of Pharmacology (NC-IUPHAR).

0223-5234/$ – see front matter © 2012 Elsevier Masson SAS. All rights reserved.
http://dx.doi.org/10.1016/j.ejmech.2012.07.021

significant problems for the treatment of urinary incontinence in clinical trial [9b], as well as no sensory effect on bladder function and no anomalous vital signs in normal subjects [9c]. On the other hand, depression effect [10a,b], hyperphasia effect [11], and blood pressure effect [12] of N/OFQ *in vivo* by way of NOP receptor–N/OFQ system have been studied, which might show the potential of NOP receptor antagonists to modulate/attenuate N/OFQ activity in pharmacological viewpoints. Therefore, potent and selective NOP receptor antagonists *per se* are also needed for investigation and recognition of N/OFQ–NOP receptor system in detail and might be useful for seeking potential pharmacological utility. Herein, the design, synthesis, and structure–activity relationship (SAR) studies of 1-(β-amino substituted-β-alanyl)-*N*,*N*-dimethylindoline-2-carboxamide derivatives for potent and selective novel NOP receptor antagonists *in vitro* with efficient analogue-developing strategy, and significant findings of the analogues are reported.

2. Results and discussion

2.1. Chemistry

For design and SAR studies of NOP receptor antagonists *in vitro*, the synthesis of various 1-(β-amino substituted-β-alanyl)-*N*,*N*-dimethylindoline-(2*RS* or 2*S*)-2-carboxamide derivatives were efficiently performed as follows.

First, a racemic compound, *tert*-butyl (2*RS*)-2-(dimethylcarbamoyl)indoline-1-carboxylate (*rac*)-**1** that was prepared from 1-(*tert*-butoxycarbonyl)indoline-(2*RS*)-2-carboxylic acid by amidation with dimethylamine, water soluble carbodiimide [1-ethyl-3-(3-dimethylaminopropylcarbodiimide) hydrochloride (WSCI)], and 1-hydroxybenzotriazole (HOBT) [13] was N-deprotected by acidic condition to afford *N*,*N*-dimethylindoline-(2*RS*)-2-carboxamide (*rac*)-**2**. The unprotected 1-amino portion of the indoline derivative (*rac*)-**2** was then amidated with acryl chroride to afford 1-acryloyl-*N*,*N*-dimethylindoline-(2*RS*)-2-carboxamide (*rac*)-**3**. Furthermore, in the same manner described above, 1-acryloyl-*N*,*N*-dimethylindoline-(2*S*)-2-carboxamide (*S*)-**3**, that is the (*S*)-enantiomer of compound (*rac*)-**3**, was prepared from the corresponding *tert*-butyl (2*S*)-2-(dimethylcarbamoyl)indoline-1-carboxylate (*S*)-**1** (Scheme 1).

Second, the requisite 1-(N-substituted β-alanyl)-*N*,*N*-dimethylindoline-2-carboxamides were prepared for the designed SAR study by Michel addition reaction [14] from the above 1-acryloyl-*N*,*N*-dimethylindoline-2-carboxamide of racemate, (*rac*)-**3** or of (*S*)-form, (*S*)-**3** with various types of amines that were obtained from commercial suppliers or in-house library or by manual synthesis. Also, the Michel addition reaction was applied to high-speed analoging (HSA) study with library-amines selected for the SAR study. Indeed, (2*RS*)-analogues **5a**–**i** were prepared from compound (*rac*)-**3** with amines **4a**–**i** by manual synthesis, and (2*RS*)-analogues **5j**–**z** were prepared from compound (*rac*)-**3** with amines **4j**–**z** by high-speed parallel synthesis, respectively, of which the various amines were 4-(phenyl, heteroaryl, cycloalkyl, and other substituted) piperidine derivatives **4a**, **4b** and **4j**–**n**, 4-(1′-aza-cycloheptanyl) phenyl derivative **4o**, 1-(phenyl, heteroaryl, cycloalkyl, and other substituted)piperazine derivatives **4c**–**i** and **4p**–**v**, and fused bi- or tri-cycloamine derivatives **4w**–**z**, respectively (Scheme 2). As well, (2*S*)-analogues **7a**–**f** were prepared from compound (*S*)-**3** with various 4-(phenyl or substituted phenyl)piperidine derivatives **6a**–**f** by manual synthesis, respectively (Scheme 3). In the structural analysis study for the isolated products **5a**–**i** and **7a**–**f**, their ^{1}H NMR spectra showed the starting materials-derived amido- and amino-portion signals with several signals attributed to their amide-bond conformers, respectively, and had no olefinic-portion signals of the Michael acceptor (*rac*)-**3** or (*S*)-**3**, respectively (see Sections 4.1.3–4.1.11 and 4.1.13–4.1.18 in the Experimental section, respectively). Overall, over two hundreds analogues were produced by this method for the study (further data not shown).

As a key amine for this study, 4-(4-fluoro-2-methylphenyl) piperidine **6d** was prepared by multistep manual synthesis similar to the known synthetic conditions for phenylpiperidine derivatives [15]. Thus, 1-benzyl-4-piperidone **8** was coupled with Grignard reagent, 4-fluoro-2-methylphenylmagnesium bromide generated from 1-bromo-4-fluoro-2-methylbenzene *in situ*, and then dehydro-olefinylation for the resulting hydroxyl compound **9** was performed by acidic condition to give 1-benzyl-4-(4-fluoro-2-methylphenyl)-1,2,3,6-tetrahydropyridine **10**. Finally, simultaneous hydrogenolysis of the N-benzyl portion and hydrogenation of the olefinic portion for compound **10** with $Pd(OH)_2$ were performed to afford requisite 4-(4-fluoro-2-methylphenyl)piperidine **6d** as a sole product (Scheme 4).

The 1-β-alanyl-*N*,*N*-dimethylindoline-2-carboxamide derivatives **5a**–**i** and **7a**–**f** prepared by manual synthesis were converted into monocitrates using citric acid in CH_2Cl_2–MeOH, respectively (see Sections 4.1.3–4.1.11 and 4.1.13–4.1.18 in the Experimental section, respectively). Also, 1-β-alanyl-*N*,*N*-dimethylindoline-2-carboxamide derivatives **5j**–**z** prepared by high-speed parallel synthesis were obtained as salt-free compounds (**5j**–**y**) or a formate (**5z**), dependent on the purification condition, respectively (see Section 4.1.20 in the Experimental section). These salts and salt-free compounds were used for SAR study with pharmacological and/or pharmacokinetic evaluations, respectively.

2.2. Design, SAR, and mechanism studies in vitro for NOP receptor antagonists

Actually, the design, synthesis, and SAR studies of 1-(β-amino substituted-β-alanyl)-*N*,*N*-dimethylindoline-2-carboxamide analogues were performed to explore and identify novel NOP receptor antagonists that have potent and selective binding affinity and potent functional antagonist activity *in vitro*. The biological assays for the *in vitro* SAR study were performed as follows. The

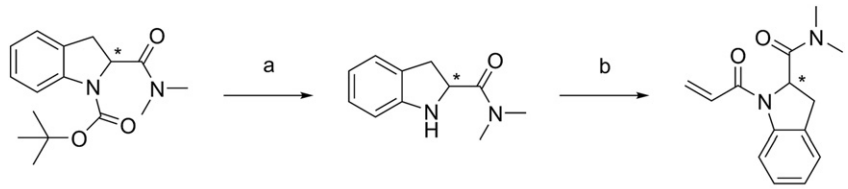

Scheme 1. Synthesis of 1-acryloyl-*N*,*N*-dimethylindoline-2-carboxamides (*rac*)-**3** and (*S*)-**3**. Reagents and conditions: (a) trifluoroacetic acid, THF, 0 °C to room temp; (b) acryloyl chloride, Et_3N, CH_2Cl_2, 0 °C.

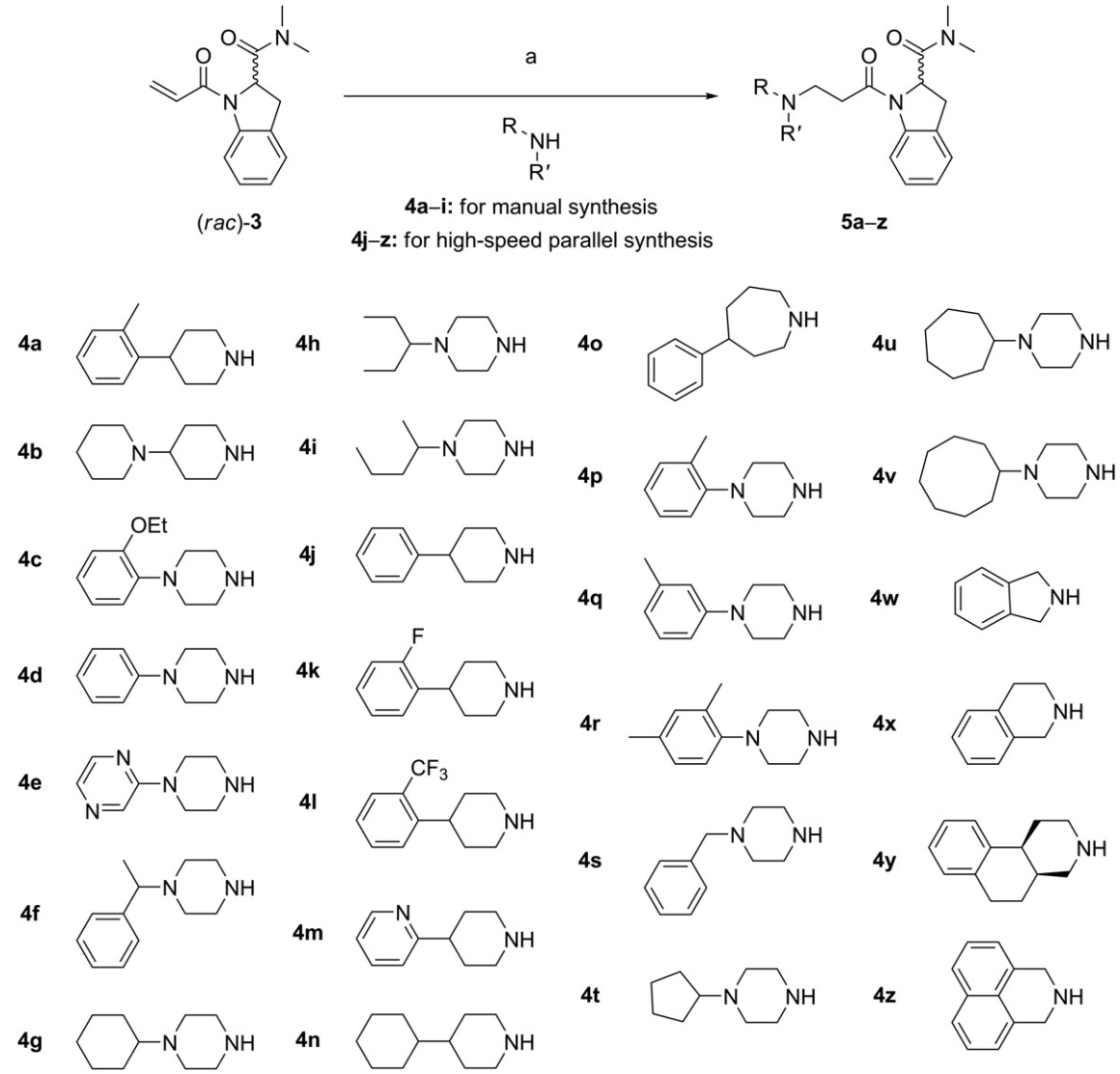

Scheme 2. Synthesis of *N*,*N*-dimethyl-1-{3-[(substituted)cycloamino]propanoyl}indoline-(2*RS*)-2-carboxamides **5a**–**z** with Michael addition reaction. Reagents and conditions: (a) Et_3N, THF, 60 °C.

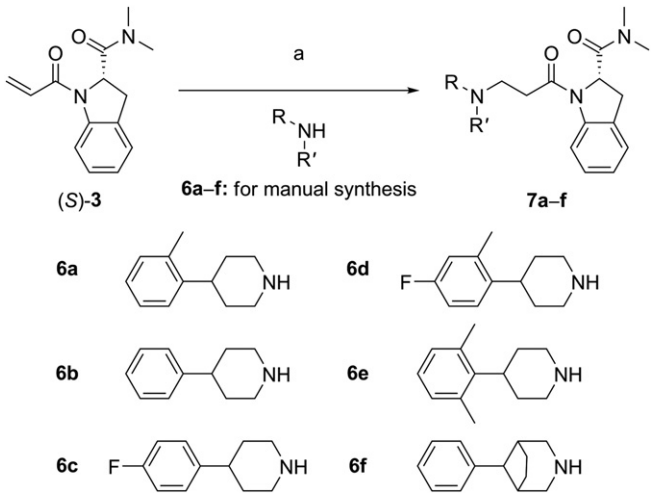

Scheme 3. Synthesis of *N*,*N*-dimethyl-1-{3-[(substituted)cycloamino]propanoyl} indoline-(2*S*)-2-carboxamides **7a**–**f** with Michael addition reaction. Reagents and conditions: (a) Et_3N, THF, 60 °C.

binding affinities (K_i values) of the synthetic analogues to human NOP (hNOP) receptor were measured by the displacement of tritium-labelled N/OFQ for the recombinant hNOP receptor expressed in human embryonic kidney (HEK)-293 cells [7,8a,16]. To

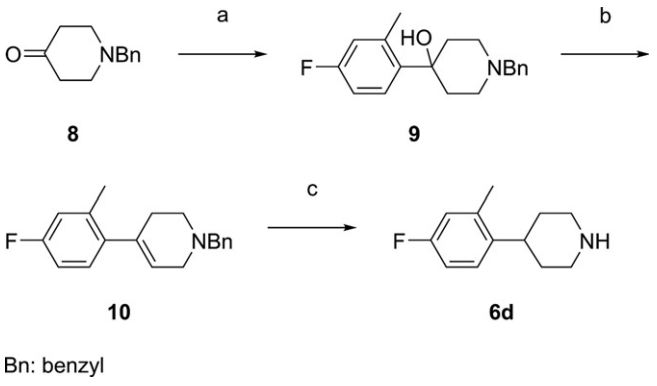

Scheme 4. Synthesis of 4-(4-fluoro-2-methylphenyl)piperidine **6d**. Reagents and conditions: (a) 4-fluoro-2-methylphenylmagnesium bromide, THF, reflux; (b) *p*-toluenesulfonic acid monohydrate, toluene, reflux; (c) $Pd(OH)_2$, MeOH, H_2 (1 atm).

evaluate *in vitro* binding selectivity of the analogues for NOP receptor over μ-opioid peptide (MOP[1]) receptor that is a classical opioid peptide receptor, the binding affinities for the analogues to human MOP (hMOP) receptor expressed in Chinese hamster ovary (CHO)-K1 cells were measured by the displacement of corresponding radiolabelled ligand, [^{3}H]DAMGO [7,8a,16]. The hNOP receptor antagonist activities of the analogues were determined as the inhibitory activities (IC_{50} values) against [^{35}S]GTPγS binding to α-unit of G-protein stimulated by N/OFQ that bound to the recombinant hNOP receptor in HEK-293 cells [7,8a].

First, synthetic 1-(N-substituted β-alanyl)-*N*,*N*-dimethylindoline-(2*RS*)-2-carboxamide derivatives, especially, aryl or heteroaryl group-substituted monocycloamine analogues, alicyclic group-substituted or acyclic-alkyl group-substituted monocycloamine analogues, fused bi- or tri-cycloamine analogues as the modification of β-amino group were explored. The results of the SAR study were illustrated in Table 1. Among this study for hNOP receptor binding affinity of the 2-racemic analogues, it was found that 4′-phenylpiperidine analogues **5a**, **5j**, **5k**, and **5l** were effective as the β-amino portion-modified analogues. In the SAR study of substituent effect on phenyl moiety of the 4′-phenylpiperidine analogues, 4′-(*ortho*-substituted phenyl)piperidine analogues were significant or tolerated for potent hNOP receptor binding affinity. And the rank of orders of the binding affinities for the various 4′-(*ortho*-substituted/unsubstituted phenyl)piperidine analogues was Me (**5a**) > H (**5j**) > F (**5k**) > CF_3 (**5l**). In particular, 4′-(*ortho*-tolyl) piperidine analogue **5a** exhibited the most potent NOP binding affinity among them, that is, the K_i value of the binding affinity to hNOP receptor was 5.55 nM, with less hMOP receptor binding affinity, that is, the K_i value was 138 nM. Further, the *ortho*-methylation of the phenyl unit was favourable for the selectivity of hNOP receptor binding over hMOP receptor binding, that is, the selectivity of 4′-(*ortho*-tolyl)piperidine analogue **5a** was 25-fold and the selectivity of 4′-(unsubstituted phenyl)piperidine analogue **5j** was 19-fold, respectively. In seeking study of other cycloamino-ring species for the corresponding piperidinyl-ring portion of the 4′-phenylpiperidine analogues, several 4′-(*ortho*-substituted phenyl) piperazine analogues were also allowed for potent binding affinities to hNOP receptor, and the rank of orders of the binding affinities for the 4′-(*ortho*-substituted/unsubstituted phenyl)piperazine analogues was Me (**5p**) > OEt (**5c**) > H (**5d**). Interestingly, compared to 4′-(*ortho*-tolyl)piperazine analogue **5p**, 4′-(*ortho*-ethoxyphenyl) piperazine analogue **5c** showed reduced hNOP receptor binding affinity ($K_i = 127$ nM) and increased hMOP receptor binding affinity ($K_i = 29.8$ nM), thus rather hMOP receptor binding selectivity (4-fold). As the SAR of cycloamino-ring portion, relative to the above 4′-(*ortho*-tolyl)piperidine analogue **5a**, 4′-(*ortho*-tolyl)piperazine analogue **5p** showed a half less potent hNOP receptor binding affinity ($K_i = 11.6$ nM) with comparative hNOP receptor binding selectivity over hMOP receptor binding ($K_i = 318$ nM), that is, the hNOP receptor selectivity for compound **5p** was 27-fold.

In the functional study *in vitro*, the above 4′-(*ortho*-tolyl)piperidine analogue **5a** and 4′-phenylpiperidine analogue **5j** exhibited hNOP receptor antagonist activities as inhibitory activities against [^{35}S]GTPγS binding induced by N/OFQ, that is, the respective IC_{50} values were 116 nM for compound **5a** and 2296 nM for compound **5j**, which were related to the degree of the respective hNOP receptor binding affinities *in vitro*. Also 4′-phenylpiperazine analogue **5d** that had very weak hNOP receptor binding affinity exhibited much less hNOP receptor antagonist activity compared to the above compounds **5a** and **5j**.

Besides, other mono- or di-methylphenyl analogues such as 4′-(*meta*-tolyl)piperazine analogue **5q**, 4′-(2″,4″-dimethylphenyl) piperazine analogue **5r**, and 4′-(3″,4″-dimethylphenyl)piperazine analogue (not shown) showed much less hNOP receptor binding

Table 1
Structure–activity relationships of *in vitro* binding affinities to human recombinant NOP receptor and human recombinant MOP receptor, and *in vitro* antagonist activities against human recombinant NOP receptor for 1-β-alanyl-*N*,*N*-dimethylindoline-(2*RS*)-2-carboxamide analogues **5a**–**z**.[a]

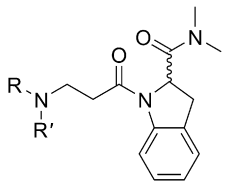

Compounds		Binding affinity K_i (nM)[b]		Antagonism against N/OFQ stimulated [^{35}S]GTPγS binding IC_{50} (nM)[c]
No	*RR′N*–	hNOP	hMOP	
5a	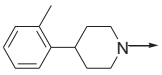	5.55	138	116
5b	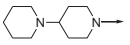	>250 (inactive @1 μM)	>450	NT[d]
5c	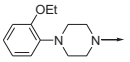	128	29.8	NT
5d	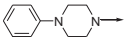	>250 (43% @1 μM)	397	48,000
5e	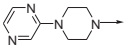	>250 (37% @1 μM)	235	NT
5f	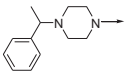	>250 (21% @1 μM)	>450	NT
5g	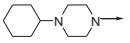	>250 (11% @1 μM)	>450	NT
5h	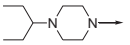	101	>450	NT
5i	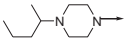	>250 (40% @1 μM)	>450	NT
5j	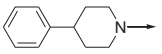	26.2	502	2296
5k	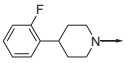	26.5	NT	NT
5l	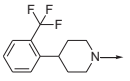	31.5	NT	NT
5m	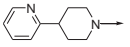	>250 (inactive @1 μM)	NT	NT
5n	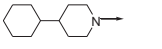	286	NT	NT
5o	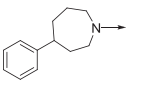	>250 (15% @1 μM)	NT	NT

(*continued on next page*)

Table 1 (*continued*)

Compounds		Binding affinity K_i (nM)[b]		Antagonism against N/OFQ stimulated [^{35}S]GTPγS binding IC_{50} (nM)[c]
No	*RR′N*–	hNOP	hMOP	
5p	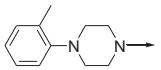	11.6	318	NT
5q	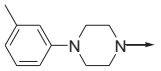	>250 (13% @1 μM)	NT	NT
5r	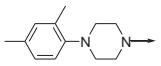	>250 (25% @1 μM)	NT	NT
5s	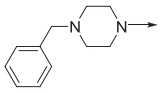	>250 (11% @1 μM)	>450	NT
5t	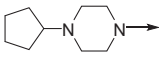	>250 (3% @1 μM)	NT	NT
5u	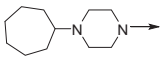	>250 (12% @1 μM)	NT	NT
5v	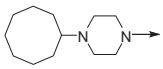	>250 (12% @1 μM)	NT	NT
5w	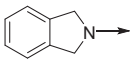	>250 (16% @1 μM)	NT	NT
5x	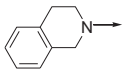	>250 (11% @1 μM)	NT	NT
5y	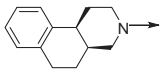	>250 (33% @1 μM)	NT	NT
5z	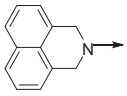	>250 (15% @1 μM)	NT	NT

[a] **5a**–**i**: products by manual synthesis; **5j**–**z**: products by high-speed parallel synthesis.

[b] K_i values for compounds were measured by displacement of [^{3}H]N/OFQ binding to hNOP receptor expressed in HEK-293 cells and of [^{3}H]DAMGO binding to hMOP receptor expressed in CHO-K1 cells, respectively. $K_i = IC_{50}/(1+[\text{radioligand}]/K_D)$. Radioligands: [^{3}H]N/OFQ as hNOP receptor agonist, concentration 0.4 nM, $K_D = 0.135$ nM; [^{3}H]DAMGO as hMOP receptor agonist, concentration 1.0 nM, $K_D = 0.821$ nM.

[c] Antagonism IC_{50} values for compounds were measured as inhibitory activity against [^{35}S]GTPγS binding to α-unit of G-protein due to binding of N/OFQ to hNOP receptor expressed in HEK-293 cells.

[d] NT, not tested.

affinity or inactivity at 1 μM. Hence, steric substituent on *meta*- or *para*-position of the phenyl group was not allowed for hNOP receptor binding, and the negative steric hindrance effect at the position(s) was also supported by other analogues (not shown). As well, heteroaryl group substitution instead of the phenyl group of the 4′-phenylpiperidine/4′-phenylpiperazine analogue, for example, 4′-(pyridin-2″-yl)piperidine analogue **5m** and 4′-(pyrazin-2″-yl)piperazine analogue **5e** gave very weak activity or inactivity at 1 μM for the hNOP receptor binding, respectively, showing electron-state (electron-density) effect for the aryl core to exhibit hNOP receptor binding affinity.

Further approaches around 1-(N-substituted β-alanyl)-*N*,*N*-dimethylindoline-2-carboxamide analogues as shown below to explore chemical space for exhibiting hNOP receptor binding affinity were not successful. Thus, (1) for 4′-position modification on piperidin-1′-yl or piperazin-1′-yl substituent as the β-amino portion, (i) alicyclic substituted-groups such as 4′-piperidinopiperidine (**5b**), 4′-cyclohexylpiperidine (**5n**), 4′-cyclopentylpiperazine (**5t**), 4′-cyclohexylpiperazine (**5g**), 4′-cycloheptylpiperazine (**5u**), and 4′-cyclooctylpiperazine (**5v**), as well as (ii) acyclic-alkyl substituted-groups such as 4′-(1″-ethylpropyl)piperazine (**5h**) and 4′-(1″-methylbutyl)piperazine (**5i**) groups gave much less activity or inactivity. (2) Ring enlargement analogue of the piperidine moiety of 4′-phenylpiperidine analogue, that is, 4′-phenyl-1′-aza-cycloheptane analogue **5o** was inactive. (3) As a modification of 4′-phenylpiperidine portion, insertion of methylene bridge between the piperidinyl ring and phenyl ring such as development to 4′-benzylpiperidine analogues **5f** and **5s**, or alkyl bridge insertion within the piperidinyl ring such as development to bicycloamine analogues (not shown, also relative analogue is discussed later) resulted in very weak activity or inactivity. (4) In case benzo-fused bi- or tri-cyclic amines (**5w**–**z**) were used as the replacement of 4′-phenylpiperidine, the affinities were much reduced, respectively. (5) In case fused bi-alicyclic amine such as decahydroisoquinoline or mono-alicyclic amine such as 1′-azacyclooctane was used for β-amino portion of β-alanine analogues, the affinities were very weak or inactive ($K_i > 250$ nM) (further data not shown).

Taken together, among the above various analogues in the SAR study, 4′-(*ortho*-methyl substituted-phenyl)piperidine analogues were the most promising/encouraging leads for further design, synthesis, and SAR development study, because of their appropriate structural features and chemical properties such as appropriate electron-state (electron-density) of the aryl (phenyl) ring core, appropriate bulkiness and electron state of the *ortho*-position substituent of phenyl ring, and preferable size/volume/bulkiness and shape of the cycloamino (piperidinyl) ring portion which contribute to their potent and selective hNOP receptor binding affinities and potent hNOP receptor antagonist activities *in vitro*.

Next, synthetic 1-(N-substituted β-alanyl)-*N*,*N*-dimethylindoline-(2*S*)-2-carboxamide derivatives, especially around 4′-phenylpiperidine analogues were designed and investigated to identify potent and selective hNOP receptor antagonists *in vitro*. The results were summarized as shown in Table 2.

As comparison between (*S*)-configuration- and racemic-forms of potent indoline amide analogues for hNOP receptor binding affinity, (*S*)-form 4′-*ortho*-tolylpiperidine analogue **7a** and 4′-phenylpiperidine analogue **7b** showed approximately twice potent binding affinities than that of the corresponding racemic analogues **5a** and **5j**, respectively, that is, the K_i values of *ortho*-tolyl analogues were 3.03 nM for (*S*)-form **7a** and 5.55 nM for racemate **5a**, respectively, and the K_i values of phenyl analogues were 13.6 nM for (*S*)-form **7b** and 26.2 nM for racemate **5j**, respectively. Furthermore, the respective hNOP receptor antagonist activities for (*S*)-forms **7a** ($IC_{50} = 44$ nM) and **7b** ($IC_{50} = 138$ nM) were more potent than the corresponding racemates **5a** and **5j**, respectively. Hence, it was clarified that (*S*)-configuration forms of these analogues were apparently preferable to the corresponding racemates for both hNOP receptor binding affinities and hNOP receptor antagonist activities, respectively. Besides the selectivities of the binding affinity to hNOP receptor over hMOP receptor for *ortho*-tolyl analogues were comparative between (*S*)-form **7a** (22-fold) and the corresponding racemate **5a** (25-fold), which were higher than that

Table 2
Structure–activity relationships of *in vitro* binding affinities to human recombinant NOP receptor and human recombinant MOP receptor, and *in vitro* antagonist activities against human recombinant NOP receptor for 1-β-alanyl-*N*,*N*-dimethylindoline-(2*S*)-2-carboxamide analogues **7a**–**f**.[a]

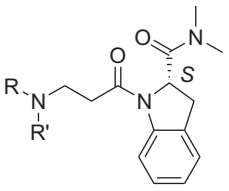

Compounds		Binding affinity K_i (nM)[b]		Antagonism against N/OFQ stimulated [^{35}S]GTPγS binding IC_{50} (nM)[c]
No	*RR′N*–	hNOP	hMOP	
7a	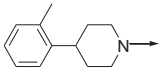	3.03	67.2	44
7b	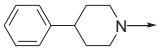	13.6	80.7	138
7c	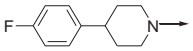	9.84	238	107
7d	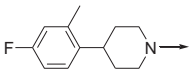	3.79	139	42
7e	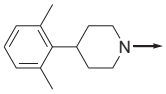	0.96	82.1	12
7f	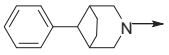	>250 (23% @1 μM)	28.4	NT[d]

[a] **7a**–**f**: products by manual synthesis.
[b] K_i values for these compounds were measured by displacement of [^{3}H]N/OFQ binding to hNOP receptor expressed in HEK-293 cells and of [^{3}H]DAMGO binding to hMOP receptor expressed in CHO-K1 cells, respectively (see also footnotes of Table 1).
[c] Antagonism IC_{50} for compounds were measured against N/OFQ-stimulated [^{35}S]GTPγS binding.
[d] NT, not tested.

of (*S*)-form 4′-phenylpiperidine analogue **7b** (5.9-fold) and the corresponding racemate **5j** (19-fold).

Therefore, further design and synthetic studies were performed around (*S*)-forms of 4′-phenylpiperidine derivatives for achieving potent and selective *in vitro* activity as hNOP receptor antagonist, as well as metabolic stability (mentioned later). Indeed, (*S*)-form 4′-(4″-fluorophenyl)piperidine analogue **7c** also showed greater hNOP receptor binding affinity (K_i = 9.84 nM) than that of (*S*)-form 4′-(unsubstituted phenyl)piperidine analogue **7b**, and further, on the basis of multi-viewpoint results (described later) of 4′-(*ortho*-tolyl) piperidine analogue **7a** and 4′-(4″-fluorophenyl)piperidine analogue **7c**, (*S*)-4′-(4″-fluoro-2″-methylphenyl)piperidine analogue **7d** was designed, which resulted in retained potency with improved selectivity: the K_i value of hNOP receptor binding affinity was 3.79 nM, and the K_i value of hMOP receptor binding affinity was 139 nM, thus the selectivity for hNOP receptor over hMOP receptor was 37-fold. Furthermore, 4′-(2″,6″-dimethylphenyl)piperidine analogue **7e** was the most potent analogue among this series of analogues, that is, the K_i value of the hNOP receptor binding affinity was 0.6 nM with 86-fold hNOP receptor selectivity over hMOP receptor. As for a bicycloamino analogue, that is, 8′-phenyl-3′-azabicyclo[3.2.1]octane analogue **7f** showed very weak hNOP receptor binding affinity and rather potent hMOP receptor binding affinity, thereby supporting profitability of the piperidine as cycloamino ring for β-portion modification of the β-alanine analogue as described already.

Significantly, the above 4′-phenylpiperidine analogues **7a**–**e** that possessed potent hNOP receptor binding affinities exhibited potent hNOP receptor antagonist activities, respectively, that is, their IC_{50} values were 12–138 nM. The potencies of the antagonist activities are depended on that of the respective hNOP receptor binding affinities for the analogues, and the relationships between them are clearer than that of the mentioned cases of the racemic 4′-phenyl(piperidine or piperazine) analogues. Thus, for hNOP receptor antagonists **7a**–**e**, there are highly significant positive correlations of their IC_{50} values against N/OFQ-stimulated [^{35}S]GTPγS binding to the respective K_i values for inhibition of [^{3}H]N/OFQ binding as shown in Fig. 1 (r^2 = 0.9911, $p < 0.0005$). In the present study, it is indicated that the binding of hNOP receptor antagonists to NOP receptor is the primary mechanism of the inhibition of G-protein activation response that is stimulated by N/OFQ. More specifically, the present data demonstrated that the appropriately modified 4′-phenylpiperidine portion, that plays an essential role for the relationships in the study, and/or the other part or whole entity of the analogue that is assisted by the 4′-phenylpiperidine portion, effectively blocks or interferes on an indispensable site or region for both the receptor binding and biological activity in the hNOP receptor protein. By contrast, as previously reported study by Hayashi et al. [8a], MCOPPB analogues {2-substituted 1-[1-(1-methylcyclooctyl)piperidin-4-yl]-1*H*-benzimidazole derivatives} as hNOP receptor agonists exhibited highly significant positive correlations of their *in vitro* EC_{50} (potency) values, that were the concentrations producing a half-maximal response of them evaluated by the [^{35}S]GTPγS binding in response to the agonist–receptor binding, to their respective *in vitro* K_i values, that were evaluated by the inhibition of [^{3}H]N/OFQ binding, indicating that the binding of hNOP receptor agonist to hNOP receptor is the primary mechanism of the G-protein activation response and the potency of the functional activity depends on the potency of the binding affinity for each analogue. And the results also demonstrated that the 2-substituent portion of the benzimidazole analogue that plays an essential role for the relationships in the study, and/or the other part or whole entity of the analogue that is assisted by the 2-substituent portion, effects on an indispensable site or region for both the receptor binding and biological activity in the hNOP receptor protein. On the other hand,

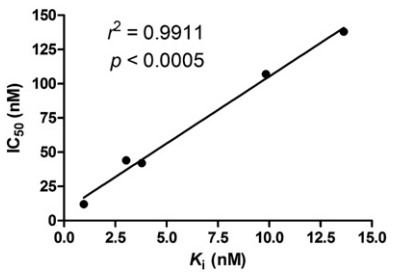

Fig. 1. Correlation between K_i and IC_{50} for human nociceptin/orphanin FQ peptide (hNOP) receptor antagonists **7a**–**e**. K_i values for binding affinity to hNOP receptor; IC_{50} values for hNOP receptor antagonist activity against nociceptin/orphanin FQ (N/OFQ)-stimulated [^{35}S]-guanosine 5′-(γ-thiotriphosphate) binding.

supported or complementally results have been reported for biological function of NOP receptor. Thus, (i) several cavities in its transmembrane regions work for binding to N/OFQ and following biological activity as a GPCR, where are able to be affected by mutation of amino acid residues around the binding site [17]. For example, one cavity in a transmembrane region works for binding to N/OFQ with biological activity, but loses the biological function after the binding if Gln^{286} of the binding site is point mutated, namely, the transduction of N/OFQ signal is not conveyed after the binding, thereby the functional switch remains off [17]. Similarly, (ii) Asn^{133} mutation of NOP receptor causes no biological response after N/OFQ binding [18]. In other words, these residues of NOP receptor in the reported studies such as (i) Gln^{286} and (ii) Asn^{133} were estimated as functionally important, respectively. Therefore, the results of the present SAR study for hNOP receptor antagonists and of the previous SAR study for hNOP receptor agonists (MCOPPB analogues as well as HPCOM analogues) [7,8], and these analogues *per se* might be quite useful to elucidate functional mechanisms of NOP receptor–ligand interactions, that includes further exploring/identifying the dynamics of intercepting (by antagonists) or causing (by N/OFQ or other agonists) effect via receptor–ligand binding on biological signal-transduction mechanisms/pathways of GPCR systems with the receptor, as well as specifying/focusing further or detailed intrinsic portion, character or pharmacophore of the receptor or the ligands in terms of biological function after the binding.

Indeed, for example, in a viewpoint of the structural feature of the β-portion substituent for the present series of β-alanine amide analogues regarding the molecular-recognition mechanisms and functional mechanisms as receptor–ligand interactions, the relationship for the position/orientation between phenyl ring and piperidinyl ring is significant, thus restriction of torsion angle (dihedral angle) of phenyl-ring plain and cycloamino-ring portion would influence on the potency of hNOP receptor binding affinity and hNOP receptor antagonist activity. Actually, when the torsion angle between two rings was restricted to (or fixed for) non-coplanar or was ranged around perpendicular because of the steric hindrance by *ortho*-substituent on phenyl ring, for example, in the cases of 4′-(*ortho*-tolyl)piperidine analogue **7a** and 4′-(2″,6″-dimethylphenyl)piperidine analogue **7e**, their respective hNOP receptor binding affinities and hNOP receptor antagonist activities that were closely correlated to the binding affinities were greater than that of 4′-phenylpiperidine analogue **7b**. On the contrary, when the phenyl ring was united/fixed with the cycloamino ring as nearly coplanar position as a whole, thus in the cases of 1′,2′,3′,4′-tetrahydroisoquinoline analogue **5x** and 1′,2′,3′,4′,4′a,5′,6′,10′b-octahydrobenzo[*f*]isoquinoline analogue **5y**, their hNOP receptor binding affinities were low or inactive. By contrast, in the case of 4′-(unsubstituted phenyl)piperidine analogue **5j**, the phenyl moiety is placed at 4′-piperidine moiety via a single bond without no significant steric hindrance, the angle between phenyl ring and cycloamino ring is freely variable, thereby showing much greater hNOP receptor binding affinity than that of 1′,2′,3′,4′,4′a,5′,6′,10′b-octahydrobenzo[*f*]isoquinoline analogue **5y** and less than that of 4′-(*ortho*-tolyl)piperidine analogue **5a**. Hence it would be estimated that the single-bond rotation between phenyl- and piperidinyl-rings for compound **5j** would allow its active conformation in the compound–hNOP receptor complex at binding mode, whereas the coplanar-like moiety consisted of phenyl- and piperidinyl-rings for compound **5y** would avoid/inhibit the active conformation.

In other structural viewpoints, it is noteworthy that the stereochemistry of the present (*S*)-configuration of hNOP receptor antagonists and previous (*R*)-configuration of hNOP receptor agonists [8a] is also important for their *in vitro* potent antagonist activities and *in vitro* potent agonist activities, respectively, which clearly shows that the stereochemistry of the antagonists/agonists is closely related to the degrees of molecular-recognition and functional-action (intercepting or causing signal transduction) of the antagonists/agonists for NOP receptor, respectively.

In conclusion, it was revealed that the respective structural features and chemical properties of the β-amino substituent of β-alanine part for the present series of analogues, such as appropriate total and partial size/volume/bulkiness, shape, and electron state (electron-density degree or electron-density distribution), the position/orientation pattern of substituent(s)/pharmacophore(s), and the stereochemical character of the molecule would deeply contribute to the underlying dynamic interaction mechanisms of hNOP receptor binding and hNOP receptor antagonism for the analogues in the biological field, which would be also related to the underlying interaction mechanisms of hNOP receptor binding and hNOP receptor function for N/OFQ or hNOP receptor agonist(s).

2.3. Design and SMR studies in vitro with multi-viewpoint integrated strategy for NOP receptor antagonists

During the course of design, synthesis, and *in vitro* SAR studies of the above (*S*)-form *N*,*N*-dimethylindoline-2-carboxamide analogues to identify potent and selective NOP receptor antagonists as described, simultaneously, design and *in vitro* structure–metabolic stability relationship (SMR) for the analogues were investigated to identify metabolically stable analogues as well, for an integrated drug-design strategy with multi-viewpoint evaluations as described already in the discovery study of orally potent anxiolytic by Hayashi et al. [8b]. For the present study, the half-lives of NOP receptor antagonists in human liver microsomes (HLMs), that is related to long duration of drug efficacy with good bioavailability [7,8b], were investigated as pharmacokinetic evaluation *in vitro*. Also, physicochemical properties for the analogues were estimated, for example, the lipophilicity value for the whole structure of the respective molecule at pH 7.4 was calculated as ACD log *D* calculated by ACD software (ACD log $D_{7.4}$). The results of the relationships of structure–metabolic stability–physicochemical properties for NOP receptor agonists were summarized in Table 3.

As described, regarding with the *in vitro* SAR study of 4′-phenylpiperidine portion of (*S*)-form *N*,*N*-dimethylindoline-2-carboxamide analogues, 4′-(*ortho*-tolyl)piperidine analogue **7a** was more potent and selective hNOP receptor antagonist compared to 4′-phenylpiperidine analogue **7b**; however, 4′-(*ortho*-tolyl) piperidine analogue **7a** showed less half-life (24 min) than that of 4′-phenylpiperidine analogue **7b** (55 min) in HLM as a result of SMR study. Besides, as a significant finding, further designed 4′-(4″-fluorophenyl)piperidine analogue **7c** prolonged half-life in HLM (82 min) compared to 4′-phenylpiperidine analogue **7b**, which might be due to blocking effect by introduction of fluorine atom against the potential metabolic site at *para*-position of the phenyl nucleus (also discussed later), with the improved *in vitro* characters as hNOP receptor antagonist relative to 4′-phenylpiperidine analogue **7b**, and comparable hNOP receptor selectivity to that of 4′-(*ortho*-tolyl)piperidine analogue **7a**. Therefore, 4′-(4″-fluoro-2″-methylphenyl)piperidine analogue **7d** was designed for the compatibility of potent and selective hNOP receptor binding affinity and potent hNOP receptor antagonist activity *in vitro*, and long half-life *in vitro*. Actually, the novel analogue **7d** achieved longer lasting half-life *in vitro* (43 min) than that of 4″-position unblocked 4′-(*ortho*-tolyl)piperidine analogue **7a**, as well as the potent and selective binding affinity, and the potent antagonist activity *in vitro* as described already.

As another side of SMR viewpoints, *ortho*-methyl substituent effect in terms of *in vitro* metabolic stability for compound **7a** relative to compound **7b** as 4′-(4″-unsubstituted phenyl)piperidine

Table 3
SAR of metabolic stabilities (half-lives in human liver microsomes) versus physicochemical properties for (*S*)-1-β-alanyl-*N*,*N*-dimethylindoline-2-carboxamide analogues **7a**–**f**.

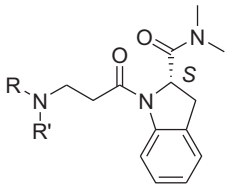

Compounds		Half-life in HLM	Physicochemical properties			
			Lipophilicity	Size	HBA[b]	TPSA[c]
No	*RR′N*–	min	ACD log $D_{7.4}$[a]	M_W	Number	Å^2
7a	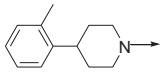	24	2.41	419.56	3	43.86
7b	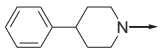	55	1.95	405.53	3	43.86
7c	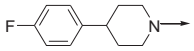	82	2.03	423.52	3	43.86
7d	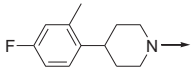	43	2.49	437.55	3	43.86
7e	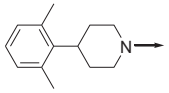	19	2.87	433.59	3	43.86
7f	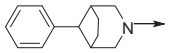	10	2.11	431.57	3	43.86

[a] Predicted by ACD/laboratories 9.0.
[b] HBA, hydrogen bond acceptor.
[c] TPSA, topological polar surface area.

analogues, and the effect for compound **7c** relative to compound **7d** as 4′-(4″-fluorophenyl)piperidine analogues were almost same, thus the *ortho*-methyl substituent, that is, more lipophilic and bulkier than hydrogen, influenced to shorten half-life in each case. As well, in comparison between 4′-phenylpiperidine analogue **7b** and 8′-phenyl-3′-azabicyclo[3.2.1]octane analogue **7f**, the latter one showed shorter half-life than that of the former one, owing to its bicycloamino moiety that is more lipophilic and bulkier than monocycloamino moiety of the former one. Besides, the major metabolic site of a 2″,6″-dimethylphenyl analogue was 4″-position of the phenyl core, which was identified as 4″-hydroxylated metabolite by HPLC–MS/MS analysis in our metabolite study with liver microsome (further data not shown). Therefore, the lipophilicity and/or steric effect, and metabolic-site protection would be estimated as key factors for the present analogues to vary metabolic stability *in vitro*. Furthermore, it is significant to consider the SMR study with a viewpoint of physicochemical property for the present series of analogues (Table 3). Thus, except 4′-(4″-fluorophenyl)piperidine analogues (**7c** and **7d**), the relationship between half-life evaluated in HLM and lipophilicity estimated as ACD log $D_{7.4}$ value for 4′-(substituted or unsubstituted phenyl) piperidine analogues (**7a**, **7b**, and **7e**), that have similarity of other structural features such as molecular weight (M_W), hydrogen-bonding functionality (for example, number of hydrogen bond acceptor), and topological polar surface area (TPSA), indicates that the degree of metabolic stability is inversely related to the degree of lipophilicity. As well, for the potential metabolic site-blocked analogues such as **7c** and **7d**, the relationship of metabolic stability–lipophilicity was the same, as mentioned above for the *ortho*-methyl substituent effect in the SMR study. Hence, the tendency of the relationship for the present series of analogues, that is, lower the lipophilicity, the longer the half-life, is in line with the previously reported results for HPCOM analogues or MCOPPB analogues by Hayashi et al. [7,8b] on condition that the other structural features or chemical properties are almost same or similar, and that the potential metabolic-site issue is removable or negligible or similar, for example, in case the major determinant-moiety of lipophilicty-difference and the major metabolic-site are located at different portions each other for the series of analogues.

In summary, as the results of the present design and SMR study, it was clarified that the important factors to achieve long-lasting metabolic stability *in vitro* for β-amino substituent of the present series of β-alanine analogues were protection of potential metabolic-reaction, low lipophilicity, and/or low steric-effect, with appropriate other structural/chemical properties. Furthermore, through the present drug-design, synthesis, SAR, and SMR studies with efficient, logical, and integrated strategy *in vitro*, 1-{3-[4-(substituted phenyl)piperidin-1-yl]propanoyl}-*N*,*N*-dimethylindoline-(2*S*)-2-carboxamide analogues were discovered as potent, selective, and long-lasting metabolically stable novel hNOP

receptor antagonists. These analogues and their SAR/SMR outcomes might be quite useful to elucidate functional mechanisms of N/OFQ–NOP receptor system *in vitro* as well as *in vivo* for further studies.

3. Conclusions

In the present drug-discovery study, 1-(β-amino substituted-β-alanyl)-*N*,*N*-dimethylindoline-(2*RS*)-2-carboxamide derivatives were explored to elucidate structural requisites for hNOP receptor antagonist activity with efficient synthesis and well-designed SAR investigation *in vitro*, which resulting in the discovery of 1-{3-[4-(substituted phenyl)piperidin-1-yl]propanoyl}-*N*,*N*-dimethylindoline-(2*RS*)-2-carboxamide analogues as novel hNOP receptor antagonists. Furthermore, simultaneous investigation of SAR and SMR *in vitro* for 1-{3-[4-(substituted phenyl)piperidin-1-yl]propanoyl}-*N*,*N*-dimethylindoline-(2*S*)-2-carboxamide analogues were very useful and effective to design and identify potent, selective, and metabolically stable hNOP receptor antagonists *in vitro*, and the significant findings are as follows: (i) The (2*S*)-form analogues were superior to the corresponding racemic analogues for hNOP receptor binding affinities and antagonist activities. (ii) There are highly significant positive correlations of the IC_{50} values to the respective K_i values for hNOP receptor antagonists **7a**–**e**, and the structural features and chemical properties of the hNOP receptor antagonists would influence on (or contribute to) their inhibition mechanisms against dynamic signal-transduction of N/OFQ–NOP receptor system. (iii) As a representative, 1-{3-[4-(4-fluoro-2-methylphenyl) piperidin-1-yl]propanoyl}-*N*,*N*-dimethylindoline-(2*S*)-2-carboxamide **7d**, that was rationally designed through the integrated SAR and SMR studies, demonstrates potent and selective hNOP receptor binding affinity, potent hNOP receptor antagonist activity, and long-lasting half-life in HLM owing to the introduction of the methyl group to restrict position and orientation (torsion angle) between the phenyl portion and the piperidinyl portion of the β-amino moiety, and to the introduction of the fluorine atom at potential metabolic-reaction site on the phenyl nucleus. Overall, the SAR/SMR outcomes for the present series of analogues and the analogues *per se* might be quite useful to elucidate further underlying functional mechanisms of N/OFQ–NOP receptor system in detail for further hNOP receptor antagonist studies as well as NOP receptor studies.

4. Experimental section

4.1. Chemistry

4.1.1. General procedures

In general, reagents, solvents, and other chemicals were used as purchased without further purification. All reactions with air- or moisture-sensitive reactants and solvents were carried out under nitrogen atmosphere. Flash column chromatography (medium pressure liquid chromatography) purifications were carried out using Merck silica gel 60 (230–400 mesh ASTM). Preparative thin-layer chromatography (PTLC) purifications were carried out on Merck silica gel 60 F_{254} precoated glass plates at a thickness of 0.5 or 1.0 mm. The structures of all isolated compounds were assured by the following techniques, such as NMR, IR, MS or elementary analysis. ^{1}H nuclear magnetic resonance (^{1}H NMR) data were determined at 270 MHz on a JNM-LA 270 (JEOL) spectrometer and at 300 MHz on a JNM-LA300 (JEOL) spectrometer. Chemical shifts are expressed in δ (ppm). ^{1}H NMR chemical shifts including several signals for major amide-bond conformers of compounds were determined relative to tetramethylsilane (TMS) as internal standard. NMR data are reported as follows: chemical shift, number of atoms, multiplicities (s, singlet; d, doublet; t, triplet; q, quartet; dd, double doublet; ddd, double double doublet; m, multiplet; and br, broadened), and coupling constants. Infrared spectra were measured by an IR-470 (Shimadzu) infrared spectrometer. Low-resolution mass spectral data (EI) were obtained on an Automass 120 (JEOL) mass spectrometer. Low-resolution mass spectral data (ESI) were obtained on a Quattro II (Micromass) mass spectrometer–Agilent 1100 HPLC system. General reagents and solvents were purchased from commercial chemical suppliers. Some amines were in-house library compounds in Pfizer Global Research & Development (PGRD) or prepared by us at PGRD, Nagoya Laboratories. The compounds **5a**–**i** and **7a**–**f** prepared by manual synthesis were used for pharmacological and/or pharmacokinetic evaluations after citrate formation using one equivalent of citric acid in MeOH–CH_2Cl_2, respectively, and the purities of the citrate salts of the compounds **5a**–**i**, **7a**–**d**, and **7f** were confirmed by elementary analysis to be within ±0.4% of calculated values before the biological evaluations, respectively. As well, the compounds **5j**–**z** prepared by high-speed parallel synthesis were used for the evaluation study as salt-free form or formate salt dependent on the purification condition of the corresponding compound, respectively.

4.1.2. 1-Acryloyl-*N*,*N*-dimethylindoline-(2*RS*)-2-carboxamide [(*rac*)-**3**]

*4.1.2.1. tert-Butyl 2-(dimethylcarbamoyl)indoline-1-carboxylate [(rac)-**1**].* To a stirred suspension of indoline-2-carboxylic acid (Sigma–Aldrich, 9.790 g, 60.00 mmol) in dioxane (130 mL)–H_2O (98.0 mL) was added 2 N NaOH (32.6 mL, 65.2 mmol) and di-*tert*-butyl dicarbonate (Boc_2O) (16.5 mL, 71.8 mmol) at 0 °C under N_2. The mixture was allowed to warm to room temperature and stirred under N_2 for 1 day. The mixture was concentrated *in vacuo*. The aqueous residue was dissolved in H_2O (total amount 130 mL), acidified by adding 10% aqueous citric acid, and extracted with AcOEt (150 mL × 2). The combined organic extracts were dried over anhydrous $MgSO_4$, concentrated *in vacuo* to afford 15.66 g of 1-(*tert*-butoxycarbonyl)indoline-(2*RS*)-2-carboxylic acid (crude) as a brownish-white solid. In the spectrum of ^{1}H NMR (270 MHz, $CDCl_3$) for the product, a broad signal of 9H proton at 1.53–1.43 ppm attributed to *tert*-butoxycarbonyl (Boc) group was confirmed, with several broad signals for other parts of the product at other positions of the chart (further data not shown; see also an NMR signal data for Boc group of compound (*rac*)-**1** as shown below).

To a stirred mixture of 1-(*tert*-butoxycarbonyl)indoline-(2*RS*)-2-carboxylic acid (15.66 g, crude) and dimethylamine hydrochloride (14.68 g, 180 mmol) in dry CH_2Cl_2 (150 mL) was added water soluble carbodiimide, that is, 1-ethyl-3-(3-dimethylaminopropyl) carbodiimide hydrochloride (WSCI) (23.00 g, 120 mmol), 1-hydroxybenzotriazole (HOBT) (16.33 g, 120 mmol), and dry Et_3N (42.0 mL, 300 mmol) at 0 °C under N_2. The mixture was allowed to room temperature and stirred under N_2 for 1 day. The mixture was poured into ice-cooled saturated aqueous $NaHCO_3$ (100 mL). The resulting mixture was shaken, and the organic layer was separated. The aqueous layer was extracted with CH_2Cl_2 (100 mL). The organic layers were combined, dried over anhydrous $MgSO_4$, and concentrated *in vacuo*. The residue was purified by flash column chromatography (silica gel, hexane/AcOEt = 1:2) to afford 11.03 g of the title product (*rac*)-**1** in 63% yield (2 steps) as a slight brownish-white solid. ^{1}H NMR (270 MHz, $CDCl_3$) δ 7.92–6.88 (4H, m, Ar H), 5.25–5.08 (1H, m, C*H*), 3.47 (1H, dd, J = 16.0 Hz, J = 11.2 Hz, CH_2), 3.18–2.93 (7H, m, CH_2 and N(CH_3)$_2$), 1.59–1.48 (9H, m, O–C(CH_3)$_3$). MS (EI direct) m/z: M^+ 290.

*4.1.2.2. N,N-Dimethylindoline-(2RS)-2-carboxamide [(rac)-**2**].* To a stirred solution of *tert*-butyl (2*RS*)-2-(dimethylcarbamoyl)indoline-1-carboxylate (*rac*)-**1** (11.03 g, 37.99 mmol) in anhydrous THF

(44.0 mL) was added trifluoroacetic acid (TFA) (133 mL) at 0 °C under N_2. The mixture was stirred at 0 °C under N_2 for 30 min, allowed to room temperature, stirred for 2 h, then concentrated *in vacuo*. The residue was dissolved in CH_2Cl_2 (150 mL)–H_2O (150 mL). The organic layer was separated, dried over anhydrous $MgSO_4$, and concentrated *in vacuo* to afford 7.15 g of the title product (*rac*)-**2** in 99% yield as a slight brownish-white solid. ^{1}H NMR (270 MHz, $CDCl_3$) δ 7.08–7.03 (2H, m, Ar H), 6.80–6.70 (2H, m, Ar H), 4.57 (1H, dd, J = 10.7 Hz, J = 5.62 Hz, C*H*), 3.50 (1H, dd, J = 15.7 Hz, J = 10.7 Hz, CH_2), 3.16 (1H, dd, J = 15.7 Hz, J = 5.62 Hz, CH_2), 3.07 (3H, s, NCH_3), 2.99 (3H, s, NCH_3).

*4.1.2.3. 1-Acryloyl-N,N-dimethylindoline-(2RS)-2-carboxamide [(rac)-**3**].* To a stirred solution of *N,N*-dimethylindoline-(2*RS*)-2-carboxamide (*rac*)-**2** (7.150 g, 37.58 mmol) in dry CH_2Cl_2 (140 mL) was added dry Et_3N (13.1 mL, 94.0 mmol) at room temperature under N_2. The mixture was cooled to 0 °C, then acryloyl chloride (3.70 mL, 45.1 mmol) was added. The reaction mixture was stirred at 0 °C under N_2 for 2 h, then poured into saturated aqueous $NaHCO_3$ (150 mL) at 0 °C. The mixture was stirred at 0 °C for 15 min, then the organic layer was separated. The aqueous layer was extracted with CH_2Cl_2 (100 mL × 2). The organic layers were combined, dried over anhydrous $MgSO_4$, and concentrated *in vacuo*. The residue was purified by flash column chromatography (silica gel, hexane/acetone = 1:1) followed by recrystallization from AcOEt–hexane to afford 5.335 g of the title product (*rac*)-**3** in 58% yield as a yellowish-white solid. ^{1}H NMR (300 MHz, DMSO-d_6) δ 8.20 (1H, d, J = 8.40 Hz, Ar H), 7.21–7.16 (2H, m, Ar H), 7.03–6.98 (1H, m, Ar H), 6.37–6.21 (2H, m, CH_2=C*H*(CO) and CH_2=CH(CO)), 5.76–5.68 (2H, m, CH_2=CH(CO) and C*H*–CON$(CH_3)_2$), 3.68 (1H, dd, J = 17.1 Hz, J = 11.1 Hz, CH_2), 3.11 (3H, s, NCH_3), 3.03 (1H, d, J = 18.3 Hz, CH_2), 2.84 (3H, s, NCH_3). MS (EI direct) m/z: M^+ 244.

*4.1.3. N,N-Dimethyl-1-[3-(4-o-tolylpiperidin-1-yl)propanoyl] indoline-(2RS)-2-carboxamide (**5a**)*

A solution of 4-*o*-tolylpiperidine hydrochloride (Arch, 52.9 mg, 0.250 mmol), compound (*rac*)-**3** (61.7 mg, 0.252 mmol), and dry Et_3N (91 μL, 0.65 mmol) in anhydrous THF (3.0 mL) was stirred at 60 °C under N_2 for 36 h, cooled to room temperature, then concentrated *in vacuo*. PTLC purification (silica gel, CH_2Cl_2/MeOH = 10:1) was performed to afford 70.9 mg of the title product **5a** in 68% yield as a solid. ^{1}H NMR (270 MHz, $CDCl_3$) δ 8.31 (0.4H, d, J = 7.72 Hz, Ar(indoline) H that is a peak for an amide-bond conformer), 7.30–7.06 (6.6H, m, Ar H including Ar(indoline) H that is a peak for an amide-bond conformer), 7.03–6.97 (1H, m, Ar(indoline) H), 5.50–5.45 (0.6H, m, C*H*–CO that is a peak for an amide-bond conformer), 5.26–5.21 (0.4H, m, C*H*–CO that is a peak for an amide-bond conformer), 3.75–2.47 (15H, m, Ar–C*H*, CH_2, and N$(CH_3)_2$), 2.29–2.11 (2H, m, CH_2), 2.34 (3H, s, Ar–CH_3), 1.87–1.74 (4H, m, CH_2). *General procedure of monocitrate formation*. A solution of compound **5a** (70.9 mg, 0.169 mmol) and one equivalent of citric acid (32.5 mg, 0.169 mmol) in dry MeOH (15.0 mL)–dry CH_2Cl_2 (12.0 mL) was stirred at room temperature under N_2 for 2 h, and then concentrated *in vacuo*. The residue was solidified from dry CH_2Cl_2–dry hexane. After removing solvent *in vacuo*, the solid was collected and dried under vacuum at 60 °C for 2 h to afford 93.1 mg of monocitrate of compound **5a** as a white solid: IR (KBr): 3398, 2932, 1724, 1655, 1485, 1406, 1261, 1123, 756, 598 cm^{-1}. Anal. ($C_{26}H_{33}N_3O_2 \cdot C_6H_8O_7$) C, H, N.

*4.1.4. 1-[3-(1,4′-Bipiperidin-1′-yl)propanoyl]-N,N-dimethylindoline-(2RS)-2-carboxamide (**5b**)*

A solution of 1,4′-bipiperidine (Sigma–Aldrich, 33.7 mg, 0.200 mmol), compound (*rac*)-**3** (48.9 mg, 0.200 mmol), and dry Et_3N (45 μL, 0.32 mmol) in anhydrous THF (3.0 mL) was stirred at 60 °C under N_2 for 36 h, cooled to room temperature, then concentrated *in vacuo*. PTLC purification (silica gel, CH_2Cl_2/MeOH/25% aqueous ammonia = 10:1:0.5) was performed to afford 71.9 mg of the title product **5b** in 87% yield. ^{1}H NMR (300 MHz, $CDCl_3$) δ 8.28 (0.4H, d, 8.25 Hz, Ar H that is a peak for an amide-bond conformer), 7.26–7.08 (2.6H, m, Ar H including a peak for an amide-bond conformer), 6.99 (1H, ddd, J = 7.32 Hz, J = 7.14 Hz, J = 1.11 Hz, Ar H), 5.47–5.44 (0.6H, C*H*–CO that is a peak for an amide-bond conformer), 5.21 (0.4H, d, 8.61 Hz, C*H*–CO that is a peak for an amide-bond conformer), 3.72–1.76 (23H, m, NC*H*$(CH_2)_2$, CH_2, and N$(CH_3)_2$), 1.69–1.38 (8H, m, CH_2). Monocitrate of compound **5b**: IR (KBr): 3396, 2943, 1653, 1597, 1483, 1406, 1271, 1123, 1061, 989, 760, 598 cm^{-1}. MS (ESI positive) m/z: $[M + H]^+$ 413.28. Anal. ($C_{24}H_{36}N_4O_2 \cdot C_6H_8O_7$) C, H, N.

*4.1.5. 1-{3-[4-(2-Ethoxyphenyl)piperazin-1-yl]propanoyl}-N,N-dimethylindoline-(2RS)-2-carboxamide (**5c**)*

A solution of 1-(2-ethoxyphenyl)piperazine monohydrochloride (Sigma–Aldrich, 48.6 mg, 0.200 mmol), compound (*rac*)-**3** (48.9 mg, 0.200 mmol), and dry Et_3N (72.5 μL, 0.52 mmol) in anhydrous THF (3.0 mL) was stirred at 60 °C under N_2 for 36 h, cooled to room temperature, then concentrated *in vacuo*. PTLC purification (silica gel, CH_2Cl_2/MeOH = 20:1) was performed to afford 61.1 mg of the title product **5c** in 68% yield. ^{1}H NMR (300 MHz, $CDCl_3$) δ 8.61 (0.4H, d, J = 7.50 Hz, Ar(indoline) H that is a peak for an amide-bond conformer), 7.29–6.83 (7.6H, m, Ar H including Ar(indoline) H that is a peak for an amide-bond conformer), 5.49–5.46 (0.6H, m, C*H*–CO that is a peak for an amide-bond conformer), 5.26–5.23 (0.4H, m, C*H*–CO that is a peak for an amide-bond conformer), 4.07 (2H, q, 6.96 Hz, OCH_2CH_3), 3.75–1.70 (20H, m, CH_2 and N$(CH_3)_2$), 1.46 (3H, t, J = 6.96 Hz, OCH_2CH_3). Monocitrate of compound **5c**: IR (KBr): 3410, 2932, 1728, 1655, 1501, 1485, 1404, 1248, 1121, 1042, 984, 935, 754, 598, 536 cm^{-1}. MS (ESI positive) m/z: $[M + H]^+$ 451.26. Anal. ($C_{26}H_{34}N_4O_3 \cdot C_6H_8O_7$) C, H, N.

*4.1.6. N,N-Dimethyl-1-[3-(4-phenylpiperazin-1-yl)propanoyl] indoline-(2RS)-2-carboxamide (**5d**)*

A solution of 1-phenylpiperazine (Tokyo Chemical Industry, 32.4 mg, 0.200 mmol), compound (*rac*)-**3** (48.9 mg, 0.200 mmol), and dry Et_3N (45 μL, 0.32 mmol) in anhydrous THF (3.0 mL) was stirred at 60 °C under N_2 for 36 h, cooled to room temperature, then concentrated *in vacuo*. PTLC purification (silica gel, CH_2Cl_2/MeOH = 20:1) was performed to afford 41.2 mg of the title product **5d** in 51% yield. ^{1}H NMR (300 MHz, $CDCl_3$) δ 8.31–8.28 (0.4H, m, Ar(indoline) H that is a peak for an amide-bond conformer), 7.29–6.83 (8.6H, m, Ar H including Ar(indoline) H that is a peak for an amide-bond conformer), 5.49–5.46 (0.6H, m, C*H*–CO that is a peak for an amide-bond conformer), 5.24–5.21 (0.4H, m, C*H*–CO that is a peak for an amide-bond conformer), 3.73–1.80 (20H, m, CH_2 and N$(CH_3)_2$). Monocitrate of compound **5d**: IR (KBr): 3418, 2932, 1728, 1655, 1599, 1485, 1402, 1250, 1124, 982, 928, 758, 696, 596, 581 cm^{-1}. MS (ESI positive) m/z: $[M + H]^+$ 407.22. Anal. ($C_{24}H_{30}N_4O_2 \cdot C_6H_8O_7$) C, H, N.

*4.1.7. N,N-Dimethyl-1-[3-(4-pyrazin-2-ylpiperazin-1-yl)propanoyl] indoline-(2RS)-2-carboxamide (**5e**)*

A solution of 1-(2-pyrazinyl)piperazine (Chess, 32.8 mg, 0.200 mmol), compound (*rac*)-**3** (48.9 mg, 0.200 mmol), and dry Et_3N (45 μL, 0.32 mmol) in anhydrous THF (3.0 mL) was stirred at 60 °C under N_2 for 36 h, cooled to room temperature, then concentrated *in vacuo*. PTLC purification (silica gel, CH_2Cl_2/MeOH = 20/1/) was performed to afford 70.1 mg of the title product **5e** in 86% yield. ^{1}H NMR (300 MHz, $CDCl_3$) δ 8.30 (0.4H, d, J = 8.40 Hz, Ar(indoline) H that is a peak for an amide-bond conformer), 8.13 (1H, m, pyrazine H), 8.06 (1H, dd, J = 2.55 Hz, J = 1.47 Hz, pyrazine H), 7.85 (1H, d, J = 2.58 Hz, pyrazine H),

7.28–7.10 (2.6H, m, Ar H including Ar(indoline) H that is a peak for an amide-bond conformer), 7.00 (1H, dd, J = 7.32 Hz, J = 6.96 Hz, Ar(indoline) H), 5.50–5.46 (0.6H, m, C*H*–CO that is a peak for an amide-bond conformer), 5.23–5.19 (0.4H, m, C*H*–CO that is a peak for an amide-bond conformer), 3.75–1.65 (20H, m, CH_2 and $N(CH_3)_2$). Monocitrate of compound **5e**: IR (KBr): 3390, 1717, 1653, 1485, 1427, 1259, 1205, 1078, 831, 758 cm^{-1}. MS (ESI positive) m/z: $[M + H]^+$ 409.21. Anal. ($C_{22}H_{28}N_6O_2 \cdot C_6H_8O_7$) C, H, N.

4.1.8. *N,N-Dimethyl-1-{3-[4-(1-phenylethyl)piperazin-1-yl] propanoyl}indoline-(2RS)-2-carboxamide (**5f**)*

A solution of 1-(1-phenylethyl)piperazine (Chess, 38.1 mg, 0.200 mmol), compound (*rac*)-**3** (48.9 mg, 0.200 mmol), and dry Et_3N (45 μL, 0.32 mmol) in anhydrous THF (3.0 mL) was stirred at 60 °C under N_2 for 36 h, cooled to room temperature, then concentrated *in vacuo*. PTLC purification (silica gel, CH_2Cl_2/MeOH = 20/1/) was performed to afford 75.4 mg of the title product **5f** in 87% yield. ^1H NMR (300 MHz, $CDCl_3$) δ 8.27 (0.4H, d, J = 7.68 Hz, Ar(indoline) H that is a peak for an amide-bond conformer), 7.33–7.07 (7.6H, m, Ar H including Ar(indoline) H that is a peak for an amide-bond conformer), 7.01–6.95 (1H, m, Ar(indoline) H), 5.46–5.43 (0.6H, m, C*H*–CO that is a peak for an amide-bond conformer), 5.24–5.19 (0.4H, m, C*H*–CO that is a peak for an amide-bond conformer), 3.70–1.73 (21H, m, *CH*CH_3, CH_2, and $N(CH_3)_2$), 1.37 (3H, d, 6.60 Hz, $CHCH_3$). Monocitrate of compound **5f**: MS (ESI positive) m/z: $[M + H]^+$ 435.26. IR (KBr): 3400, 2934, 1717, 1655, 1483, 1406, 1269, 1123, 760, 706, 600 cm^{-1}. Anal. ($C_{26}H_{34}N_4O_2 \cdot C_6H_8O_7$) C, H, N.

4.1.9. *1-[3-(4-Cyclohexylpiperazin-1-yl)propanoyl]-N,N-dimethylindoline-(2RS)-2-carboxamide (**5g**)*

A solution of 1-cyclohexylpiperazine (Acros, 33.7 mg, 0.200 mmol), compound (*rac*)-**3** (48.9 mg, 0.200 mmol), and dry Et_3N (45 μL, 0.32 mmol) in anhydrous THF (3.0 mL) was stirred at 60 °C under N_2 for 48 h, cooled to room temperature, then concentrated *in vacuo*. PTLC purification (silica gel, CH_2Cl_2/MeOH/25% aqueous ammonia = 10:1:0.5) was performed to afford 67.5 mg of the title product **5g** in 82% yield as a white solid. ^1H NMR (300 MHz, $CDCl_3$) δ 8.24 (0.4H, d, J = 8.04 Hz, Ar H that is a peak for an amide-bond conformer), 7.22–7.04 (2.6H, m, Ar H including a peak for an amide-bond conformer), 6.94 (1H, ddd, J = 7.50 Hz, J = 7.14 Hz, J = 1.26 Hz, Ar H), 5.43–5.39 (0.6H, m, C*H*–CO that is a peak for an amide-bond conformer), 5.18–5.14 (0.4H, m, C*H*–CO that is a peak for an amide-bond conformer), 3.68–0.99 (31H, m, N*CH*$(CH_2)_2$, CH_2, and $N(CH_3)_2$). Monocitrate of compound **5g**: IR (KBr): 3410, 2937, 2860, 1719, 1649, 1483, 1406, 1121, 1080, 943, 758, 598 cm^{-1}. MS (ESI positive) m/z: $[M + H]^+$ 413.28. Anal. ($C_{24}H_{36}N_4O_2 \cdot C_6H_8O_7$) C, H, N.

4.1.10. *1-{3-[4-(1-Ethylpropyl)piperazin-1-yl]propanoyl}-N,N-dimethylindoline-(2RS)-2-carboxamide (**5h**)*

A solution of 1-(3-pentyl)piperazine (Chess, 31.3 mg, 0.200 mmol), compound (*rac*)-**3** (48.9 mg, 0.200 mmol), and dry Et_3N (45 μL, 0.32 mmol) in anhydrous THF (3.0 mL) was stirred at 60 °C under N_2 for 48 h, then cooled to room temperature. The reaction solution was poured into H_2O, and the mixture was extracted with CH_2Cl_2 twice. The combined extracts were dried over anhydrous $MgSO_4$, and then concentrated *in vacuo*. PTLC purification (silica gel, CH_2Cl_2/MeOH/25% aqueous ammonia = 10:1:0.05) was performed to afford 67.8 mg of the title product **5h** in 85% yield as a white solid. ^1H NMR (300 MHz, $CDCl_3$) δ 8.28 (0.4H, d, J = 8.25 Hz, Ar H that is a peak for an amide-bond conformer), 7.26–7.08 (2.6H, m, Ar H including a peak for an amide-bond conformer), 6.98 (1H, ddd, J = 7.35 Hz, J = 7.32 Hz, J = 1.11 Hz, Ar H), 5.47–5.43 (0.6H, m, C*H*–CO that is a peak for an amide-bond conformer), 5.23–5.19 (0.4H, m, C*H*–CO that is a peak for an amide-bond conformer), 3.72–2.37 (20H, m, CH_2 and $N(CH_3)_2$), 2.13 (1H, quintet, 6.42 Hz, N*CH*$(CH_2CH_3)_2$), 1.56–1.24 (4H, m, NCH$(CH_2CH_3)_2$), 0.89 (6H, t, 7.50 Hz, NCH$(CH_2CH_3)_2$). Monocitrate of compound **5h**: IR (KBr): 3414, 2966, 2936, 1720, 1655, 1597, 1483, 1406, 1271, 1123, 758, 598 cm^{-1}. MS (ESI positive) m/z: $[M + H]^+$ 401.24. Anal. ($C_{23}H_{36}N_4O_2 \cdot C_6H_8O_7$) C, H, N.

4.1.11. *N,N-Dimethyl-1-{3-[4-(1-methylbutyl)piperazin-1-yl] propanoyl}indoline-(2RS)-2-carboxamide (**5i**)*

A solution of 1-(2-pentyl)piperazine (Chess, 31.3 mg, 0.200 mmol), compound (*rac*)-**3** (48.9 mg, 0.200 mmol), and dry Et_3N (45 μL, 0.32 mmol) in anhydrous THF (3.0 mL) was stirred at 60 °C under N_2 for 48 h, then cooled to room temperature. The reaction solution was poured into H_2O, extracted with CH_2Cl_2 twice. The combined extracts were dried over anhydrous $MgSO_4$, and then, concentrated *in vacuo*. PTLC purification (silica gel, CH_2Cl_2/MeOH/25% aqueous ammonia = 10:1:0.05) was performed to afford 62.0 mg of the title product **5i** in 77% yield as a white solid. ^1H NMR (300 MHz, $CDCl_3$) δ 8.28 (0.5H, d, J = 8.07 Hz, Ar H that is a peak for an amide-bond conformer), 7.25–7.09 (2.5H, m, Ar H including a peak for an amide-bond conformer), 6.98 (1H, ddd, J = 7.53 Hz, J = 7.14 Hz, J = 1.08 Hz, Ar H), 5.45 (0.5H, dd, J = 10.8 Hz, J = 3.51 Hz, C*H*–CO that is a peak for an amide-bond conformer), 5.22 (0.5H, d, J = 10.8 Hz, C*H*–CO that is a peak for an amide-bond conformer), 3.71–0.84 (31H, m, N*CH*(CH_3) CH_2, CH_2, CH_3, and $N(CH_3)_2$). Monocitrate of compound **5i**: IR (KBr): 3437, 2961, 1720, 1655, 1483, 1271, 758, 600 cm^{-1}. MS (ESI positive) m/z: $[M + H]^+$ 401.27. Anal. ($C_{23}H_{36}N_4O_2 \cdot C_6H_8O_7$) C, H, N.

4.1.12. *1-Acryloyl-N,N-dimethyl-2,3-dihydro-1H-indole-(2S)-2-carboxamide [(S)-**3**]*

1-(*tert*-Butoxycarbonyl)indoline-(2*S*)-2-carboxylic acid, that was prepared from indoline-(2*S*)-2-carboxylic acid (Tokyo Chemical Industry) by *tert*-butoxycarbonyl (Boc) protection as the above described manner, was amidated into *tert*-butyl (2*S*)-2-(dimethylcarbamoyl)indoline-1-carboxylate (*S*)-**1** in the same manner for compound (*rac*)-**1** except the temperature for the amidation reagents-adding condition was −20 °C instead of 0 °C at the corresponding synthetic protocol for compound (*rac*)-**1** (see Section 4.1.2.1.). Then compound (*S*)-**1** was converted into *N,N*-dimethyl-2,3-dihydro-1*H*-indole-(2*S*)-2-carboxamide (*S*)-**2** in the same manner for compound (*rac*)-**2** (see Section 4.1.2.2.). To a stirred solution of compound (*S*)-**2** (11.07 g, 58.19 mmol) and dry Et_3N (17.8 mL, 128 mmol) in dry CH_2C1_2 (200 mL) was added acryloyl chloride (4.98 mL, 61.3 mmol) at 0 °C under N_2. The reaction mixture was stirred at 0 °C under N_2 for 2 h, then poured into ice-cooled saturated aqueous $NaHCO_3$. The resulting mixture was extracted with CH_2C1_2, and the combined extracts were dried over anhydrous Na_2SO_4, filtered, and concentrated. The residue was purified by column chromatography (silica gel, hexane/acetone = 2:1 to 1:1) to give 8.00 g of title product (*S*)-**3** in 56% yield as a white solid. This compound showed a broadened spectrum in ^1H NMR. MS (EI direct) m/z: M^+ 244 (see also Section 4.1.2.1. for the above procedure of (*rac*)-**3**).

4.1.13. *N,N-Dimethyl-1-[3-(4-o-tolylpiperidin-1-yl)propanoyl] indoline-(2S)-2-carboxamide (**7a**)*

A solution of 4-*o*-tolylpiperidine hydrochloride (Arch, 76.2 mg, 0.360 mmol), compound (*S*)-**3** (87.9 mg, 0.360 mmol), and dry Et_3N (131 μL, 0.94 mmol) in anhydrous THF (4.4 mL) was stirred at 60 °C under N_2 for 36 h, cooled to room temperature, then concentrated *in vacuo*. PTLC purification (silica gel, CH_2Cl_2/MeOH = 10:1) was performed to afford 121.0 mg of the title product **7a** in 80% yield as a solid. ^1H NMR data of this compound **7a** was the same as that of the corresponding (*RS*)-form **5a**. Monocitrate of compound **7a**: IR data of this salt was the same as that of the corresponding

monocitrate of compound **5a**. Anal. ($C_{26}H_{33}N_3O_2 \cdot C_6H_8O_7$) C, H, N (see also Section 4.1.3. for the above ^{1}H NMR and IR data).

4.1.14. N,N-Dimethyl-1-[3-(4-phenylpiperidin-1-yl)propanoyl] indoline-(2S)-2-carboxamide (**7b**)

A solution of 1-phenylpiperidine hydrochloride (71.2 mg, 0.360 mmol), compound (*S*)-**3** (87.9 mg, 0.360 mmol), and dry Et_3N (131 μL, 0.936 mmol) in anhydrous THF (4.4 mL) was stirred at 60 °C under N_2 for 36 h, then concentrated *in vacuo*. PTLC purification (silica gel, CH_2Cl_2/MeOH = 10:1) was performed to afford 110.2 mg of the title product **7b** in 75% yield as a white solid. ^{1}H NMR (300 MHz, $CDCl_3$) δ 8.31–8.29 (0.4H, m, Ar(indoline) H that is a peak for an amide-bond conformer), 7.33–7.09 (7.6H, m, Ar H including Ar(indoline) H that is a peak for an amide-bond conformer), 7.02–6.97 (1H, m, Ar(indoline) H), 5.49–5.44 (0.6H, m, C*H*–CO that is a peak for an amide-bond conformer), 5.26–5.21 (0.4H, m, C*H*–CO that is a peak for an amide-bond conformer), 3.73–2.75 (13H, m, Ar–C*H*, CH_2, and $N(CH_3)_2$), 2.58–2.46 (2H, m, CH_2), 2.25–2.10 (2H, m, CH_2), 1.90–1.71 (4H, m, CH_2). Monocitrate of compound **7b**: IR (KBr): 3422, 2932, 1732, 1653, 1485, 1406, 1271, 1217, 1123, 758, 702, 598 cm^{-1}. Anal. ($C_{25}H_{31}N_3O_2 \cdot C_6H_8O_7$) C, H, N.

4.1.15. 1-{3-[4-(4-Fluorophenyl)piperidin-1-yl]propanoyl}-N,N-dimethylindoline-(2S)-2-carboxamide (**7c**)

A solution of 4-(4-fluorophenyl)piperidine hydrochloride (41.4 mg, 0.192 mmol), compound (*S*)-**3** (46.4 mg, 0.190 mmol), and dry Et_3N (69 μL, 0.50 mmol) in anhydrous THF (2.3 mL) was stirred at 60 °C under N_2 for 36 h, cooled to room temperature, then concentrated *in vacuo*. PTLC purification (silica gel, CH_2Cl_2/MeOH = 10:1) was performed to afford 58.9 mg of the title product **7c** in 73% yield as a solid. ^{1}H NMR (300 MHz, $CDCl_3$) δ 8.30 (0.4H, d, *J* = 8.07 Hz, Ar(indoline) H that is a peak for an amide-bond conformer), 7.29–6.94 (7.6H, m, Ar H including Ar(indoline) H that is a peak for an amide-bond conformer), 5.49–5.44 (0.6H, m, C*H*–CO that is a peak for an amide-bond conformer), 5.25–5.20 (0.4H, m, C*H*–CO that is a peak for an amide-bond conformer), 3.75–2.75 (13H, m, Ar–C*H*, CH_2, $N(CH_3)_2$), 2.55–2.46 (2H, m, CH_2), 2.23–2.11 (2H, m, CH_2), 1.88–1.69 (4H, m, CH_2). Monocitrate of compound **7c**: IR (KBr): 3400, 2932, 1719, 1655, 1485, 1406, 1221, 1123, 835, 758, 592, 540 cm^{-1}. Anal. ($C_{25}H_{30}N_3O_2F \cdot C_6H_8O_7$) C, H, N.

4.1.16. 1-{3-[4-(4-Fluoro-2-methylphenyl)piperidin-1-yl] propanoyl}-N,N-dimethylindoline-(2S)-2-carboxamide (**7d**)

A solution of 4-(4-fluoro-2-methylphenyl)piperidine (compound **6d**, see Section 4.1.19; 42.5 mg, 0.220 mmol), compound (*S*)-**3** (53.7 mg, 0.220 mmol), and dry Et_3N (56 μL, 0.40 mmol) in anhydrous THF (4.0 mL) was stirred at 60 °C under N_2 for 2 days, then cooled to room temperature, then concentrated *in vacuo*. PTLC purification (silica gel, CH_2Cl_2/MeOH = 10:1) was performed to afford 58.6 mg of the title product **7d** in 61% yield. ^{1}H NMR (300 MHz, $CDCl_3$) δ 8.30 (0.4H, d, *J* = 8.04 Hz, Ar(indoline) H that is a peak for an amide-bond conformer), 7.29–7.10 (3.6H, m, Ar H including Ar(indoline) H that is a peak for an amide-bond conformer), 7.00 (1H, dd, *J* = 7.32 Hz, *J* = 7.32 Hz, Ar H), 6.88–6.82 (2H, m, Ar H), 5.49–5.44 (0.6H, m, C*H*–CO that is a peak for an amide-bond conformer), 5.26–5.21 (0.4H, m, C*H*–CO that is a peak for an amide-bond conformer), 3.75–2.45 (15H, m, Ar–C*H*, CH_2, and $N(CH_3)_2$), 2.32 (3H, s, Ar–CH_3), 2.27–2.11 (2H, m, CH_2), 1.83–1.73 (4H, m, CH_2). Monocitrate of compound **7d**: IR (KBr): 3414, 2930, 1728, 1655, 1485, 1410, 1246, 1126, 955, 758, 594 cm^{-1}. MS (ESI positive) *m*/*z*: $[M + H]^+$ 438. Anal. ($C_{26}H_{32}N_3O_2F \cdot C_6H_8O_7$) C, H, N.

4.1.17. 1-{3-[4-(2,6-Dimethylphenyl)piperidin-1-yl]propanoyl}-N,N-dimethylindoline-(2S)-2-carboxamide (**7e**)

A solution of 4-(2,6-dimethylphenyl)piperidine (16.6 mg, 0.0880 mmol), compound (*S*)-**3** (19.1 mg, 0.0782 mmol), and dry Et_3N (17.4 μL, 0.125 mmol) in anhydrous THF (1.5 mL) was stirred at 60 °C under N_2 for 3 days, cooled to room temperature, then concentrated *in vacuo*. The residue was diluted with CH_2Cl_2 (40 mL), washed with ice-cooled saturated aqueous $NaHCO_3$ (30 mL). The organic layer was separated and the aqueous layer was extracted with CH_2Cl_2 (30 mL × 2). The organic layers were combined, dried over anhydrous $MgSO_4$, and concentrated *in vacuo*. PTLC purification was performed twice (first, silica gel, CH_2Cl_2/MeOH = 16:1; second, silica gel, CH_2Cl_2/MeOH/25% aqueous ammonia = 10:1:0.05) to afford 9.4 mg of the title product **7e** in 28% yield. ^{1}H NMR (300 MHz, $CDCl_3$) δ 8.31 (0.4H, d, *J* = 8.61 Hz, Ar(indoline) H that is a peak for an amide-bond conformer), 7.30–6.98 (6.6H, m, Ar H including Ar(indoline) H that is a peak for an amide-bond conformer), 5.50–5.42 (0.6H, m, C*H*–CO that is a peak for an amide-bond conformer), 5.30–5.21 (0.4H, m, C*H*–CO that is a peak for an amide-bond conformer), 3.75–2.09 (23H, m, Ar–C*H*, CH_2, $N(CH_3)_2$, and Ar–CH_3), 1.69–1.60 (4H, m, CH_2). MS (ESI positive) *m*/*z*: $[M + H]^+$ 434.29 for salt-free compound **7e**. Compound **7e** was converted into the corresponding monocitrate as usual, and the salt was used for pharmacological and pharmacokinetic evaluations without elementary analysis because of the requisite amount for the analysis; the purity of the salt-free compound **7e** was assured by the above ^{1}H NMR analysis that had no significant impurity signal except small amounts of solvent signal.

4.1.18. N,N-Dimethyl-1-[3-(8-phenyl-3-azabicyclo[3.2.1]oct-3-yl) propanoyl]indoline-(2S)-2-carboxamide (**7f**)

A solution of 8-phenyl-3-azabicyclo[3.2.1]octane [36.6 mg, 0.195 mmol; ^{1}H NMR (270 MHz, $CDCl_3$) δ 7.38–7.15 (5H, m), 3.12–3.07 (3H, m), 2.60–2.55 (2H, m), 2.44 (2H, dd, *J* = 12.4 Hz, *J* = 3.13 Hz), 2.02–1.80 (4H, m), 1.64 (1H, br s)], compound (*S*)-**3** (47.6 mg, 0.195 mmol), and dry Et_3N (43 μL, 0.31 mmol) in anhydrous THF (2.4 mL) was stirred at 60 °C under N_2 for 36 h, cooled to room temperature, then concentrated *in vacuo*. PTLC purification (silica gel, CH_2Cl_2/MeOH = 10:1) was performed to afford 60.2 mg of the title product **7g** in 72% yield as a solid. ^{1}H NMR (300 MHz, $CDCl_3$) δ 8.25 (0.4H, d, *J* = 7.32 Hz, Ar(indoline) H that is a peak for an amide-bond conformer), 7.34–7.08 (7.6H, m, Ar H including Ar(indoline)H that is a peak for an amide-bond conformer), 7.00–6.95 (1H, m, Ar H), 5.43–5.38 (0.6H, m, C*H*–CO that is a peak for an amide-bond conformer), 5.10–5.04 (0.4H, m, C*H*–CO that is a peak for an amide-bond conformer), 3.65–1.68 (23H, m, C*H*, CH_2, and $N(CH_3)_2$). Monocitrate of compound **7f**: IR (KBr): 2955, 1719, 1655, 1485, 1406, 1123, 993, 754 cm^{-1}. Anal. ($C_{27}H_{33}N_3O_2 \cdot C_6H_8O_7$) C, H, N.

4.1.19. Preparation of 4-(4-fluoro-2-methylphenyl)piperidine

4.1.19.1. 1-Benzyl-4-(4-fluoro-2-methylphenyl)-1,2,3,6-tetrahydropyridine (*10*). A mixture of Mg (turnings, 48.6 mg, 2.00 mmol), 1-bromo-4-fluoro-2-methylbenzene (Tokyo Chemical Industry, 253 μL, 2.00 mmol), iodine (25.4 mg, 0.100 mmol), and $MgBr_2$ (7.0 μL, 0.10 mmol) in anhydrous THF (5.0 mL) was stirred under reflux conditions under N_2 for 1 h, and cooled to room temperature. To the resulting solution of Grignard reagent (4-fluoro-2-methylphenylmagnesium bromide) was added a solution of 1-benzyl-4-piperidone (Tokyo Chemical Industry, 371 μL, 2.00 mmol) in anhydrous THF (7.0 mL) at room temperature under N_2 within 5 min. The mixture was stirred at room temperature under N_2 for 10 min, then stirred under reflux conditions for 6 h. The reaction solution was cooled to 0 °C then poured into ice-cooled aqueous NH_4Cl (40 mL). The mixture was extracted with CH_2Cl_2 (40 × 4), then the combined extracts were dried over anhydrous $MgSO_4$ and concentrated *in vacuo* to afford 658.5 mg of 1-benzyl-4-(4-fluoro-2-methylphenyl)piperidin-4-ol **9** (crude). TLC: R_f = 0.4, AcOEt/hexane = 1:8.

To a stirred solution of 1-benzyl-4-(4-fluoro-2-methylphenyl) piperidin-4-ol **9** (658.5 mg, crude) in toluene (50.0 mL) was added

p-toluenesulfonic acid monohydrate (760.1 mg, 4.00 mmol) under N_2 at room temperature. The resulting solution was heated to reflux and stirred under N_2 for 10 h. The solution was cooled to 0 °C, basified by adding 2 N NaOH (30 mL), then the mixture was extracted with chloroform (50 mL × 2). The combined extracts was dried over anhydrous $MgSO_4$, and concentrated *in vacuo*. The residue was purified by flash column chromatography (silica gel, CH_2Cl_2/MeOH = 36:1) to afford 343.3 mg of the title product **10** in 61% yield (2 steps) as a yellow oil. ^{1}H NMR (270 MHz, $CDCl_3$) δ 7.40–7.24 (5H, m, Ar H), 7.05 (1H, dd, J = 8.24 Hz, J = 6.10 Hz, Ar H), 6.88–6.77 (2H, m, Ar H) 5.53–5.49 (1H, m, C*H*), 3.65 (2H, s, Ph–CH_2–N), 3.13 (2H, dd, 5.91 Hz, 2.81 Hz, N–CH_2), 2.68 (2H, t, 5.62 Hz, N–CH_2), 2.36–2.29 (2H, m, CH_2), 2.28 (3H, s, Ar–CH_3).

*4.1.19.2. 4-(4-Fluoro-2-methylphenyl)piperidine (**6d**).* A mixture of 1-benzyl-4-(4-fluoro-2-methylphenyl)-1,2,3,6-tetrahydropyridine **10** (343.3 mg, 1.220 mmol) and $Pd(OH)_2$ (177.0 mg) in MeOH (13.0 mL) was stirred at room temperature under H_2 at 1 atm for 2 days. The catalyst was filtered through a Celite pad with MeOH. The filtrate was concentrated *in vacuo* to afford 167.5 mg of the title product **6d** in 71% yield as a white solid. ^{1}H NMR (300 MHz, $CDCl_3$) δ 7.21–7.16 (1H, m, Ar H), 6.90–6.84 (2H, m, Ar H), 3.59 (1H, br s, N*H*), 3.33 (2H, d, J = 12.3 Hz, CH_2), 2.88–2.77 (3H, m, C*H*, CH_2), 2.33 (3H, s, Ar-CH_3), 1.82–1.69 (4H, m, CH_2).

4.1.20. High-speed parallel synthesis using Michael addition reaction

(1) Reaction. To a half-dram vial, in which reagent amine or its hydrochloride (0.050 mmol) was pre-weighed, were added 0.65 mL of a 0.1 M solution of 1-acryloyl-*N*,*N*-dimethylindoline-2-carboxamide (*rac*)-**3** in 3.75% dry Et_3N–anhydrous THF and 0.25 mL of 3.75% dry Et_3N/dry dimethylacetamide and the resulting mixture was shaken at 60 °C for 16 h. After cooling to room temperature, the reaction mixture was loaded onto an Oasis MCX cartridge (1 g/6 mL) preconditioned 8 mL of MeOH. The solid-phase matrix was washed with 10 mL of MeOH and then eluted with 5 mL of 1 M ammonia/MeOH. The elute was concentrated to dryness by vacuum centrifuge, providing crude product. In case it is needed, the crude material was purified with preparative LS/MS to give the desired product as salt-free form or formic acid salt dependent on the purification condition. (2) HPLC/LC–MS method. (i) Analytical condition: equipment, Waters 2795; column: Waters XTerra C18, 5 μm, 4.6 × 50 mm; column temperature, 40 °C; detector, photodiodearray (210–400 nm); flow, 1.0 mL/min; solvent (a) as acidic condition, A: 0.1% HCO_2H; B: MeOH, gradient, solvent (b) as basic condition, A: 0.1% aqueous ammonia; B: MeOH, gradient; MS condition (ionization method), ESI (positive). (ii) Preparative conditions: equipment, Waters prep LC/MS system; column, Waters XTerra C18, 5 μm, 20 × 50 mm; column temperature, ambient temperature; flow, 20.0 mL/min; solvent (a) as acidic condition, A: 0.1% HCO_2H; B: MeOH, gradient, solvent (b) as basic condition, A: 0.1% aqueous ammonia; B: MeOH, gradient.

Utilizing the above protocol (1) and (2), parallel synthesis was performed for the analogues including **5j**–**z** (as salt-free forms of **5j**–**y** or a formate salt of **5z**) that were prepared from compound (*rac*)-**3** and the corresponding amines **4j**–**z**, respectively, as listed below:

N,*N*-Dimethyl-1-[3-(4-phenylpiperidin-1-yl)propanoyl]indoline-(2*RS*)-2-carboxamide (**5j**) (salt free) from 4-phenylpiperidine (**4j**);

1-{3-[4-(2-Fluorophenyl)piperidin-1-yl]propanoyl}-*N*,*N*-dimethylindoline-(2*RS*)-2-carboxamide (**5k**) (salt free) from 4-(2-fluorophenyl)piperidine (**4k**);

N,*N*-Dimethyl-1-(3-{4-[2-(trifluoromethyl)phenyl]piperidin-1-yl}propanoyl)indoline-(2*RS*)-2-carboxamide (**5l**) (salt free) from 4-[2-(trifluoromethyl)phenyl]piperidine (**4l**);

N,*N*-Dimethyl-1-[3-(4-pyridin-2-ylpiperidin-1-yl)propanoyl] indoline-(2*RS*)-2-carboxamide (**5m**) (salt free) from 2-(piperidin-4-yl)pyridine (**4m**);

1-[3-(4-Cyclohexylpiperidin-1-yl)propanoyl]-*N*,*N*-dimethylindoline-(2*RS*)-2-carboxamide (**5n**) (salt free) from 4-cyclohexylpiperidine (**4n**);

N,*N*-Dimethyl-1-[3-(4-phenylazepan-1-yl)propanoyl]indoline-(2*RS*)-2-carboxamide (**5o**) (salt free) from 4-phenylazepane (**4o**);

N,*N*-Dimethyl-1-[3-(4-*o*-tolylpiperazin-1-yl)propanoyl]indoline-(2*RS*)-2-carboxamide (**5p**) (salt free) from 1-*o*-tolylpiperazine (**4p**);

N,*N*-Dimethyl-1-[3-(4-*m*-tolylpiperazin-1-yl)propanoyl]indoline-(2*RS*)-2-carboxamide (**5q**) (salt free) from 1-*m*-tolylpiperazine (**4q**);

1-{3-[4-(2,4-Dimethylphenyl)piperazin-1-yl]propanoyl}-*N*,*N*-dimethylindoline-(2*RS*)-2-carboxamide (**5r**) (salt free) from 1-(2,4-dimethylphenyl)piperazine (**4r**);

1-[3-(4-Benzylpiperazin-1-yl)propanoyl]-*N*,*N*-dimethylindoline-(2*RS*)-2-carboxamide (**5s**) (salt free) from 1-benzylpiperazine (**4s**);

1-[3-(4-Cyclopentylpiperazin-1-yl)propanoyl]-*N*,*N*-dimethylindoline-(2*RS*)-2-carboxamide (**5t**) (salt free) from 1-cyclopentylpiperazine (**4t**);

1-[3-(4-Cycloheptylpiperazin-1-yl)propanoyl]-*N*,*N*-dimethylindoline-(2*RS*)-2-carboxamide (**5u**) (salt free) from 1-cycloheptylpiperazine (**4u**);

1-[3-(4-Cyclooctylpiperazin-1-yl)propanoyl]-*N*,*N*-dimethylindoline-(2*RS*)-2-carboxamide (**5v**) (salt free) from 1-cyclooctylpiperazine (**4v**);

1-[3-(Isoindolin-2-yl)propanoyl]-*N*,*N*-dimethylindoline-(2*RS*)-2-carboxamide (**5w**) (salt free) from isoindoline (**4w**);

1-{3-[3,4-Dihydroisoquinolin-2(1*H*)-yl]propanoyl}-*N*,*N*-dimethylindoline-(2*RS*)-2-carboxamide (**5x**) (salt free) from 1,2,3,4-tetrahydroisoquinoline (**4x**);

1-(3-{1,2,4,4a,5,6-*cis*-Hexahydrobenzo[*f*]isoquinolin-3(10b*H*)-yl} propanoyl)-*N*,*N*-dimethylindoline-(2*RS*)-2-carboxamide (**5y**) (salt free) from 1,2,3,4,4a,5,6,10b-*cis*-octahydrobenzo[*f*]isoquinoline (**4y**);

1-(3-{1*H*-Benzo[*de*]isoquinolin-2(3*H*)-yl}propanoyl)-*N*,*N*-dimethylindoline-(2*RS*)-2-carboxamide (**5z**) (formate) from 2,3-dihydro-1*H*-benzo[*de*]isoquinoline (**4z**).

4.2. Biology

4.2.1. In vitro characterization of NOP receptor antagonists

In vitro studies of synthetic compounds for hNOP receptor binding affinities and hMOP receptors binding affinities, and for antagonist activities against N/OFQ stimulated [^{35}S]GTPγS binding were conducted.

4.2.1.1. Materials. The hNOP receptor transfected human embryonic kidney (HEK)-293 cell membranes and the hMOP receptor transfected Chinese hamster ovary (CHO)-K1 cell membranes were purchased from Receptor Biology Inc., respectively. [^{3}H]N/OFQ (150 Ci/mmol), [^{35}S]GTPγS (1060–1150 Ci/mmol) and wheatgerm agglutinin (WGA)-scintillation proximity assay (SPA) beads were obtained from Amersham Pharmacia Biotech K.K., and [^{3}H]DAMGO (54.0 Ci/mmol) was provided from NEN™ Life Science Products Inc., respectively. N/OFQ was from Peptide Institute Inc. DAMGO was from Sigma Chemical, respectively.

4.2.1.2. Evaluation of receptor binding affinities to hNOP receptor and hMOP receptor. All competitive displacement analyses (IC_{50} and K_i) for the hNOP receptor and hMOP receptor were performed in duplicate in a 96-well plate using a scintillation proximity assay (SPA), respectively. After the reaction, the assay plate was

centrifuged at 1000 rpm for 1 min, and then the radioactivity was measured by a 1450 MicroBeta™ (Wallac) liquid scintillation counter. IC_{50} values were calculated by nonlinear regression with the software GraphPad Prism version 4.0 (GraphPad Software, Inc., San Diego, USA), respectively. K_i values were calculated by the following equation, $K_i = IC_{50}/(1 + [L]/K_D)$, where $[L]$ is the radiolabelled ligand concentration and K_D is the dissociation constant [7,8a,16].

4.2.1.2.1. hNOP receptor binding assay. The hNOP receptor membranes (8.3 μg) were incubated at 25 °C for 45 min with 0.4 nM [^{3}H]N/OFQ, 1.0 mg of WGA-SPA beads, and six different concentrations of compounds (10^{-11}–10^{-5} M, 10-fold) in a final volume of 0.2 mL of 50 mM HEPES buffer, pH 7.4, containing 10 mM $MgCl_2$ and 1 mM EDTA. Non-specific binding was determined by the addition of 1 μM unlabelled N/OFQ. Approximately 900 cpm of total binding were obtained, of which 3.3% was the non-specific binding.

4.2.1.2.2. hMOP receptor binding assay. The hMOP receptor membranes (18 μg) were incubated at 25 °C for 45 min with 1.0 nM [^{3}H]DAMGO, 1.0 mg of WGA-SPA beads, and six different concentrations of compounds (10-fold) in a final volume of 0.2 mL of 50 mM Tris–HCl buffer, pH 7.4, containing 5 mM $MgCl_2$. Non-specific binding was determined by the addition of 1 μM of unlabelled DAMGO. Approximately 240 cpm of total binding were obtained, of which 9.6% was the non-specific binding.

4.2.1.3. Evaluation of antagonist activity against N/OFQ-stimulated. [^{35}S]GTPγS binding. [^{35}S]GTPγS binding to the hNOP receptor expressed HEK-293 cell membranes was performed according to the method of SPA G-protein-coupled receptor assay provided by Amersham Biosciences with slight modification. For evaluation of antagonism activities (IC_{50}), the membranes were incubated at 25 °C for 1.5 h with 10 nM N/OFQ and various concentration of compounds in assay buffer (400 pM [^{35}S]GTPγS, 5 μM GDP, 20 mM HEPES, 100 mM NaCl, 5 mM $MgCl_2$, 1 mM EDTA, pH 7.4) containing 1.5 mg of WGA-SPA beads in a final volume of 200 μL. All assays were performed in duplicate. Each compound was tested at six different concentrations ranging from 0.1 nM to 10 μM. Membrane-bound radioactivity was detected by scintillation counting using Wallac 1450 MicroBeta™. Basal binding was determined in the absence of ligands and non-specific binding (NSB) was determined by the addition of unlabelled 10 μM GTPγS. Percent basal was defined as (stimulated binding − NSB)/(basal binding − NSB) × 100%. IC_{50} value of each compound against 10 nM N/OFQ stimulated-binding was calculated by nonlinear regression with GraphPad Prism version 4.0, respectively [7,8a].

4.3. Pharmacokinetic study

4.3.1. General

The apparatus of HPLC system was Agilent 1100 HPLC system, and, MS/MS system was API-300 or API-3000. The analytical column was YMC polymer 18, 2.0 × 75 mm. The mobile phase consisted of 10 mM aqueous $AcONH_4$ and CH_3CN (20:80, v/v) or of 0.05% aqueous TFA and CH_3CN (20:80, v/v) was run at a flow rate of 0.35 mL/min. The column temperature was at 40 °C (ambient temperature with air conditioning, 24–25 °C). The sample in column eluent was detected by MS/MS.

4.3.2. Metabolic half-life values in human liver microsomes

Test compounds (1.0 μM) were incubated in human liver microsomes (pooled human liver microsomes; protein concentration: 1.0 mg/mL) with 3.3 mM $MgCl_2$, 0.1 M $NaKHPO_4$ (pH 7.4) and NADPH-regenerating factors at 37 °C for various times on 96-deep well plates (final volume 600 μL). An aliquot of samples (50 μL) was collected at 0, 5, 15, 30, and 60 min after incubation and extracted with CH_3CN. The extracted samples were measured by HPLC/MS/MS system [7,8b].

4.4. Physicochemistry

The lipophilicity values of NOP receptor antagonists were estimated as values of ACD log $D_{7.4}$, the octanol–water distribution coefficient for ionizable compounds at pH 7.4, calculated by ACD software, ACD/Laboratories 9.0 (Advanced Chemistry Development, Inc., Ontario, Canada).

Acknowledgement

We thank chemical technology group in PGRD for technical support to our HSA study.

Appendix A. Supplementary data

Supplementary data associated with this article can be found in the online version, at http://dx.doi.org/10.1016/j.ejmech.2012.07.021. These data include MOL files and InChiKeys of the most important compounds described in this article.

References

[1] (a) J.-C. Meunier, C. Mollereau, L. Toll, C. Suaudeau, C. Moisand, P. Alvinerie, J.-L. Butour, J.-C. Guillemot, P. Ferrara, B. Monsarrat, H. Mazarguil, G. Vassart, M. Parmentier, J. Costentin, Isolation and structure of the endogenous agonist of opioid receptor-like ORL1 receptor, Nature 377 (1995) 532–535;
(b) R.K. Reinscheid, H.-P. Nothacker, A. Bourson, A. Ardati, R.A. Henningsen, J.R. Bunzow, D.K. Grandy, H. Langen, F.J.J. Monsma, O. Civelli, Orphanin FQ: a neuropeptide that activates an opioid-like G protein-coupled receptor, Science 270 (1995) 792–794.

[2] (a) K. Fukuda, S. Kato, K. Mori, M. Nishi, H. Takeshima, N. Iwabe, T. Miyata, T. Houtani, T. Sugimoto, cDNA cloning and regional distribution of a novel member of the opioid receptor family, FEBS Lett. 343 (1994) 42–46;
(b) C. Mollereau, M. Parmentier, P. Mailleux, J.-L. Butour, C. Moisand, P. Chalon, D. Caput, G. Vassart, J.-C. Meunier, ORL1, a novel member of the opioid receptor family. Cloning, functional expression and localization, FEBS Lett. 341 (1994) 33–38.

[3] (a) A. Berthele, S. Platzer, D. Dworzak, J. Schadrack, B. Mahal, A. Büttner, H.P. Aßmus, K. Wurster, W. Zieglgänsberger, B. Conrad, T.R. Tölle, [^{3}H]-Nociceptin ligand-binding and nociceptin opioid receptor mRNA expression in the human brain, Neuroscience 121 (2003) 629–640;
(b) J. Witta, M. Palkovits, J. Rosenberger, B.M. Cox, Distribution of nociceptin/orphanin FQ in adult human brain, Brain Res. 997 (2004) 24–29;
(c) K.E. Bridge, A. Wainwright, K. Reilly, K.R. Oliver, Autoradiographic localization of ^{125}I[Tyr^{14}] nociceptin/orphanin FQ binding sites in macaque primate CNS, Neuroscience 118 (2003) 513–523;
(d) L.J. Sim-Selley, L.J. Vogt, S.R. Childers, B.A. Vogt, Distribution of ORL-1 receptor binding and receptor-activated G-proteins in rat forebrain and their experimental localization in anterior cingulate cortex, Neuropharmacology 45 (2003) 220–230;
(e) J.R. Nicholson, S.J. Paterson, J.R.W. Menzies, A.D. Corbett, A.T. McKnight, Pharmacological studies on the "orphan" opioid receptor in central and peripheral sites, Can. J. Physiol. Pharmacol. 76 (1998) 304–313;
(f) L.M.E. Pettersson, F. Sundler, N. Danielsen, Expression of orphanin FQ/nociceptin and its receptor in rat peripheral ganglia and spinal cord, Brain Res. 945 (2002) 266–275;
(g) . Review: C. Mollereau, L. Mouledous, Tissue distribution of the opioid receptor-like (ORL1) receptor Peptide 21 (2000) 907–917;
(h) . Review: G. Calo', R. Guerrini, A. Rizzi, S. Salvadori, D. Regoli, Pharmacology of nociceptin and its receptor: a novel therapeutic target Br. J. Pharmacol. 129 (2000) 1261–1283;
(i) . Review: J.S. Mogil, G.W. Pasternak, The molecular and behavioral pharmacology of the orphanin FQ/nociceptin peptide and receptor family Pharmacol. Rev. 53 (2001) 381–415.

[4] (a) T. Sakurada, T. Komatsu, T. Moriyama, M. Sasaki, K. Sanai, T. Orito, C. Sakurada, S. Sakurada, Effects of intraplantar injections of nociceptin and its N-terminal fragments on nociceptive and desensitized responses induced by capsaicin in mice, Peptides 26 (2005) 2505–2512;
(b) N. Nozaki-Taguchi, T. Yamamoto, Spinal opioid receptor like1 receptor agonist, but not *N*-methyl-D-aspartic acid antagonist, reverses the secondary mechanical allodynia induced by intradermal injection of capsaicin in rats, Anesth. Analg. 100 (2005) 1087–1092;
(c) T. Yamamoto, N. Nozaki-Taguchi, S. Kimura, Effects of intrathecally administered nociceptin, an opioid receptor-like1 (ORL1) receptor agonist, on

the thermal hyperalgesia induced by carageenan injection into the rat paw, Brain Res. 754 (1997) 329–332;
(d) X. Fu, Y.-Q. Wang, G.-C. Wu, Involvement of nociceptin/orphanin FQ and its receptor in electroacupuncture-produced anti-hyperalgesia in rats with peripheral inflammation, Brain Res. 1078 (2006) 212–218;
(e) M.C.H. Ko, N.N. Naughton, J.R. Traynor, M.S. Song, J.H. Woods, K.C. Rice, A.T. McKnight, Orphanin FQ inhibits capsaicin-induced thermal nociception in monkeys by activation of peripheral ORL1 receptors, Br. J. Pharmacol. 135 (2002) 943–950;
(f) M.C.H. Ko, H. Wei, J.H. Woods, R.T. Kennedy, Effects of intrathecally administered nociceptin/orphanin FQ in monkeys: behavioral and mass spectrometric studies, J. Pharmacol. Exp. Ther. 318 (2006) 1257–1264;
(g) T. Yamamoto, N. Nozaki-Taguchi, S. Kimura, Effects of intrathecally administered nociceptin, an opioid receptor-like$_1$ (ORL$_1$) receptor agonist, on the thermal hyperalgesia induced by unilateral constriction injury to the sciatic nerve in the rat, Neurosci. Lett. 224 (1997) 107–110;
(h) T. Yamamoto, N. Nozaki-Taguchi, Effects of intrathecally administered nociceptin, an opioid receptor-like1 receptor agonist, and *N*-methyl-D-aspartate receptor antagonists on the thermal hyperalgesia induced by partial sciatic nerve injury in the rat, Anesthesiology 87 (1997) 1145–1152;
(i) J.-X. Hao, I.S. Xu, Z. Wiesenfeld-Hallin, X.-J. Xu, Anti-hyperalgesic and anti-allodynic effects of intrathecal nociceptin/orphanin FQ in rats after spinal cord injury, peripheral nerve injury and inflammation, Pain 76 (1998) 385–393;
(j) C. Courteix, M.-A. Coudoré-Civiale, A.-M. Privat, T. Pélissier, A. Eschalier, J. Fialip, Evidence for an exclusive antinociceptive effect of nociceptin/orphanin FQ, an endogenous ligand for the ORL1 receptor, in two animal models of neuropathic pain, Pain 110 (2004) 236–245;
(k) I.S. Xu, S. Grass, Z. Wiesenfeld-Hallin, X.-J. Xu, Effects of intrathecal orphanin FQ on a flexor reflex in the rat after inflammation or peripheral nerve section, Eur. J. Pharmacol. 370 (1999) 17–22;
(l) T. Yamamoto, Y. Sakashita, The role of the spinal opioid receptor like1 receptor, the NK-1 receptor, and cyclooxygenase-2 in maintaining post-operative pain in the rat, Anesth. Analg 89 (1999) 1203–1208;
(m) see also Ref. [7] by Hayashi et al. for the cited references of neuropathic pain, and for the mechanisms of analgesic activities of N/OFQ.

[5] (a) F. Jenck, J.-L. Moreau, J.R. Martin, G.J. Kilpatrick, R.K. Reinscheid, F.J.J. Monsma, H.P. Nothacker, O. Civelli, Orphanin FQ acts as an anxiolytic to attenuate behavioral responses to stress, Proc. Natl. Acad. Sci. U. S. A. 94 (1997) 14854–14858;
(b) A. Köster, A. Montkowski, S. Schulz, E.-M. Stübe, K. Knaudt, F. Jenck, J.-L. Moreau, H.-P. Nothacker, O. Civelli, R.K. Reinscheid, Targeted disruption of the orphanin FQ/nociceptin gene increases stress susceptibility and impairs stress adaptation in mice, Proc. Natl. Acad. Sci. U. S. A. 96 (1999) 10444–10449;
(c) G. Griebel, G. Perrault, D.J. Sanger, Orphanin FQ, a novel neuropeptide with anti-stress-like activity, Brain Res. 836 (1999) 221–224;
(d) F. Jenck, A.M. Ouagazzal, M. Pauly-Evers, J.-L. Moreau, Orphanin FQ: role in behavioral fear responses and vulnerability to stress? Mol. Psychiatry 5 (2000) 572–574;
(e) S. Meis, Nociceptin/orphanin FQ: actions within the brain, Neuroscientist 9 (2003) 158–168;
(f) R.K. Reinscheid, O. Civelli, The orphanin FQ/nociceptin knockout mouse: a behavioral model for stress responses, Neuropeptides 36 (2002) 72–76;
(g) A.-M. Ouagazzl, J.-L. Moreau, M. Pauly-Evers, F. Jenck, Impact of environmental housing conditions on the emotional responses of mice deficient for nociceptin/orphanin FQ peptide precursor gene, Behav. Brain Res. 144 (2003) 111–117;
(h) G.G. Blakley, L.A. Pohorecky, D. Benjamin, Behavioral and endocrine changes following antisense oligonucleotide-induced reduction in the rat NOP receptor, Psychopharmacology 171 (2004) 421–428;
(i) see also Ref. [8a,8b] by Hayashi et al. for the cited references of anxiety disorders, and for the mechanisms of anxiolytic activities of N/OFQ.

[6] (a) R. Ciccocioppo, A. Fedeli, D. Economidou, F. Policani, F. Weiss, M. Massi, The bed nucleus is a neuroanatomical substrte for the anorectic effect of corticotropin-releasing factor and for its reversal by nociceptin/orphanin FQ, J. Neurosci. 23 (2003) 9445–9451;
(b) R. Ciccocioppo, A. Cippitelli, D. Economidou, A. Fedeli, M. Massi, Nociceptin/orphanin FQ acts as a functional antagonist of corticotropin-releasing factor to inhibit its anorectic effect, Physiol. Behav. 82 (2004) 63–68.

[7] S. Hayashi, E. Nakata, A. Morita, K. Mizuno, K. Yamamura, A. Kato, K. Ohashi, Discovery of {1-[4-(2-{hexahydropyrrolo[3,4-*c*]pyrrol-2(1*H*)-yl}-1*H*-benzimidazol-1-yl)piperidin-1-yl]cyclooctyl}methanol, systemically potent novel non-peptide agonist of nociceptin/orphanin FQ receptor as analgesic for the treatment of neuropathic pain: design, synthesis, and structure–activity relationships, Bioorg. Med. Chem. 18 (2010) 7675–7699.

[8] (a) S. Hayashi, A. Hirao, A. Imai, H. Nakamura, Y. Murata, K. Ohashi, E. Nakata, Novel non-peptide nociceptin/orphanin FQ receptor agonist, 1-[1-(1-methylcyclooctyl)-4-piperidinyl]-2-[(3*R*)-3-piperidinyl]-1*H*-benzimidazole: design, synthesis, and structure–activity relationship of oral receptor occupancy in the brain for orally potent antianxiety drug, J. Med. Chem. 52 (2009) 610–625;
(b) S. Hayashi, A. Hirao, H. Nakamura, K. Yamamura, K. Mizuno, H. Yamashita, Discovery of 1-[1-(1-methylcyclooctyl)-4-piperidinyl]-2-[(3*R*)-3-piperidinyl]-1*H*-benzimidazole: integrated drug-design and structure–activity relationships for orally potent, metabolically stable and potential-risk reduced novel non-peptide nociceptin/orphanin FQ receptor agonist as antianxiety drug, Chem. Biol. Drug Des. 74 (2009) 369–381.

[9] (a) S. Giuliani, A. Lecci, M. Tramontana, C.A. Maggi, The inhibitory effect of nociceptin on the micturition reflex in anaesthetized rats, Br. J. Pharmacol. 124 (1998) 1566–1572;
(b) M. Lazzeri, G. Caló, M. Spinelli, S. Malaguti, R. Guerrini, S. Salvadori, P. Beneforti, D. Regoli, D. Turini, Daily intravesical instillation of 1 mg nociceptin/orphanin FQ for the control of neurogenic detrusor overactivity: a multicenter, placebo controlled, randomized exploratory study, J. Urol. 176 (2006) 2098–2102;
(c) M. Lazzeri, G. Calò, M. Spinelli, R. Guerrini, P. Beneforti, S. Sandri, A. Zanollo, D. Regoli, D. Turini, Urodynamic and clinical evidence of acute inhibitory effects of intravesical nociception/orphanin FQ on detrusor overactivity in humans: a pilot study, J. Urol. 166 (2001) 2237–2240.

[10] (a) E.C. Gavioli, G. Marzola, R. Guerrini, R. Bertorelli, S. Zucchini, T.C.M. De Lima, G.A. Rae, S. Salvadori, D. Regoli, G. Calo, Blockade of nociceptin/orphanin FQ–NOP receptor signalling produces antidepressant-like effects: pharmacological and genetic evidences from the mouse forced swimming test, Eur. J. Neurosci. 17 (2003) 1987–1990;
(b) E.C. Gavioli, C.W. Vaughan, G. Marzola, R. Guerrini, V.A. Mitchell, S. Zucchini, T.C.M. De Lima, G.A. Rae, S. Salvadori, D. Regoli, G. Calo', Antidepressant-like effects of the nociceptin/orphanin FQ receptor antagonist UFP-101: new evidence from rats and mice, Naunyn-Schmiedeberg's Arch. Pharmacol. 369 (2004) 547–553.

[11] D. Economidou, F. Policani, T. Angellotti, M. Massi, T. Terada, R. Ciccocioppo, Effect of novel NOP receptor ligands on food intake in rats, Peptides 27 (2006) 775–783.

[12] E. Hashiba, K. Hirota, T. Kudo, G. Calo', R. Guerrini, A. Matsuki, Effects of nociceptin/orphanin FQ receptor ligands on blood pressure, heart rate, and plasma catecholamine concentrations in guinea pigs, Naunyn-Schmiedeberg's Arch. Pharmacol. 367 (2003) 342–347.

[13] F.M. Martin, R.P. Beckett, C.L. Bellamy, P.F. Courtney, S.J. Davies, A.H. Drummond, R. Dodd, L.M. Pratt, S.R. Patel, M.L. Ricketts, R.S. Todd, A.R. Tunffnell, J.W.S. Ward, M. Whittaker, The synthesis and biological evaluation of non-peptidic matrix metalloproteinase inhibitors, Bioorg. Med. Chem. Lett. 9 (1999) 2887–2892.

[14] B.C. Hamper, S.A. Kolodziej, A.M. Scates, R.G. Smith, E. Cortez, Solid phase synthesis of β-peptoids: N-substituted β-aminopropionic acid oligomers, J. Org. Chem. 63 (1998) 708–718.

[15] S. Sakamuri, I.J. Enyedy, A.P. Kozikowski, W.A. Zaman, K.M. Johnson, S. Wang, Pharmacophore-based discovery, synthesis, and biological evaluation of 4-phenyl-1-arylalkyl piperidines as dopamine transporter inhibitors, Bioorg. Med. Chem. Lett. 11 (2001) 495–500.

[16] Y.-C. Cheng, W.H. Prusoff, Relationship between the inhibition constant (K_i) and the concentration of inhibitor which causes 50 per cent inhibition (I_{50}) of an enzymatic reaction, Biochem. Pharmacol. 22 (1973) 3099–3108.

[17] L. Mouledous, C.M. Topham, C. Moisand, C. Mollereau, J.-C. Meunier, Functional inactivation of the nociceptin receptor by alanine substitution of glutamine 286 at the C terminus of transmembrane segment VI: evidence from a site-directed mutagenesis study of the ORL1 receptor transmembrane-binding domain, Mol. Pharmacol. 57 (2000) 495–502.

[18] K.W.L. Kam, D.C. New, Y.H. Wong, Constitutive activation of the opioid receptor-like (ORL$_1$) receptor by mutation of Asn133 to tryptophan in the third transmembrane region, J. Neurochem. 83 (2002) 1461–1470.